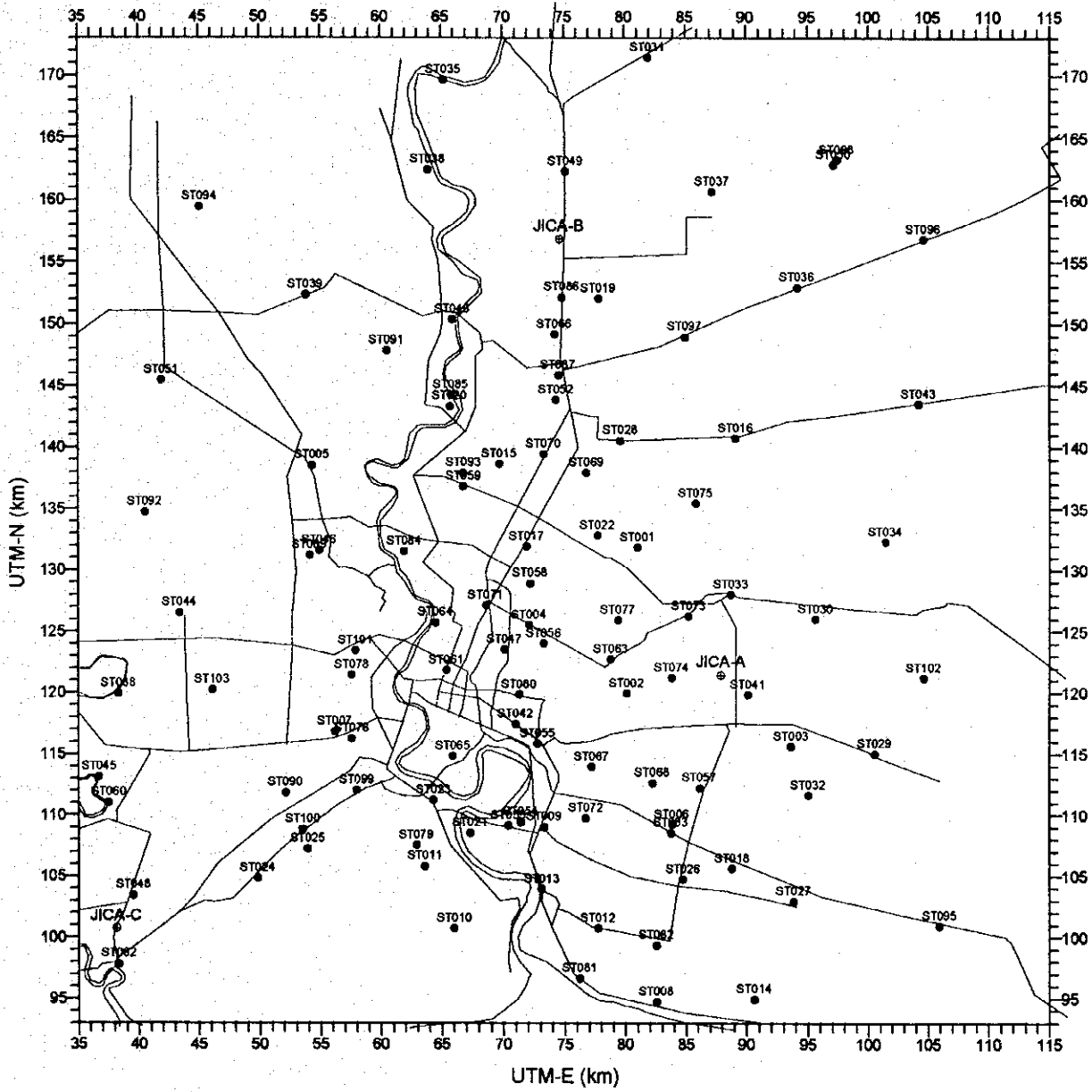


6.2.2 Land Subsidence

The DMR Survey Division started leveling survey at the DMR benchmarks as well as some of the CI stations ("AIT station" called by the DMR Survey Division) benchmarks in 1991. But the survey in 1991 covered limited benchmarks so that a subsidence map can be prepared using only the data in 1992 and 1993.

Figure 6.2.8 shows land subsidence from 1992 to 1993 measured at the DMR 1m depth benchmarks. The maximum land subsidence of 64.8 mm was recorded at DMR41 benchmark in station No. 95, Bang Bo, Samut Prakan. The areas where the subsidence is more than 40 mm can be found in Samut Prakan and eastern Bangkok. On the other hand, the northern part of the study area were rebounded during the period. It is should be noted that the rates of subsidence along the Chao Phraya River are smaller, ranging from 0 to 20 mm/year.



LEGEND

- ⊙ Location of JICA monitoring station
- Location of DMR monitoring station with station No.

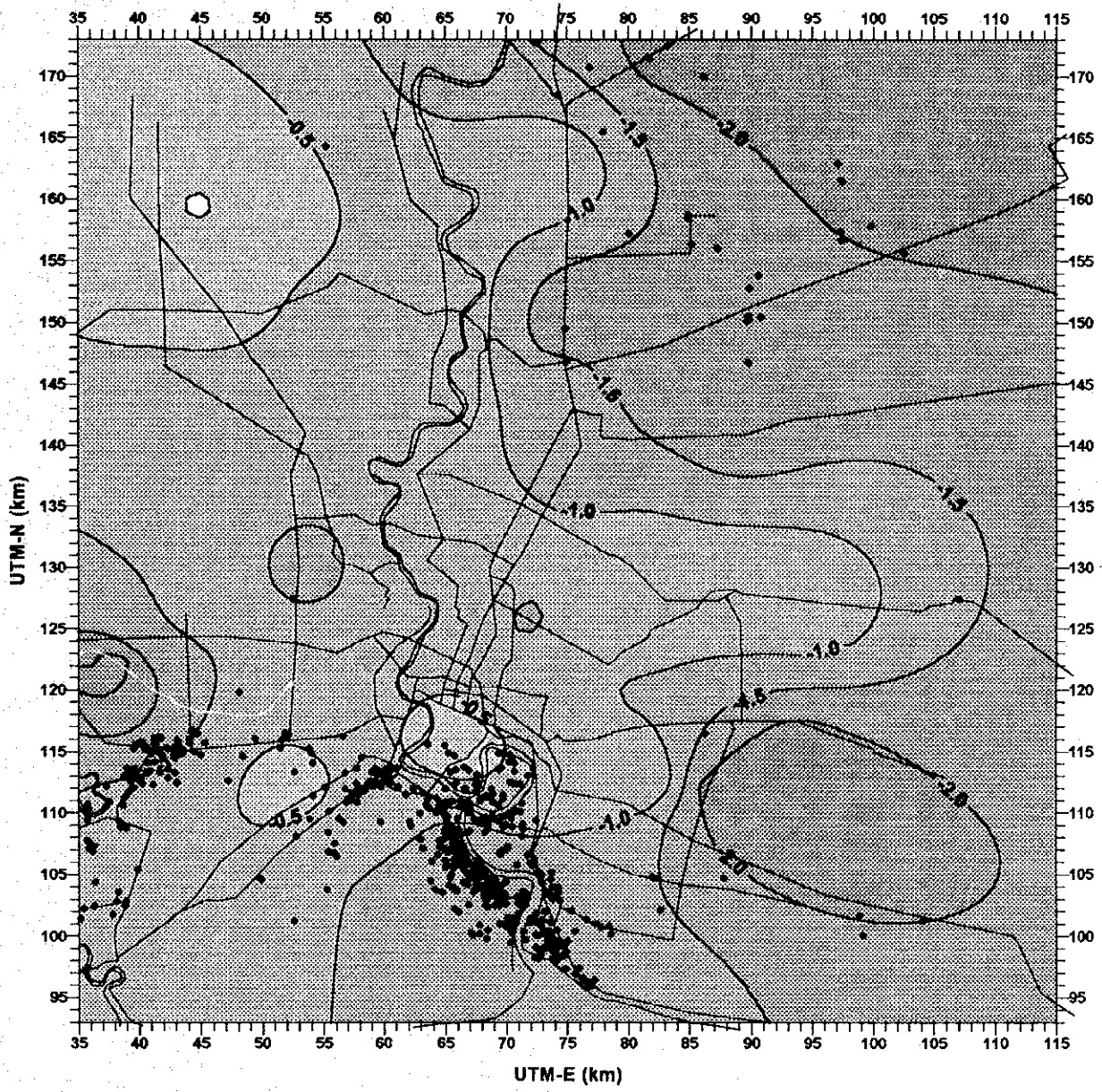
Figure 6.2.1	LOCATION OF DMR MONITORING STATIONS
THE STUDY ON MANAGEMENT OF GROUNDWATER AND LAND SUBSIDENCE IN THE BANGKOK METROPOLITAN AREA AND ITS VICINITY	
JAPAN INTERNATIONAL COOPERATION AGENCY (JICA)	KOKUSAI KOGYO CO., LTD.



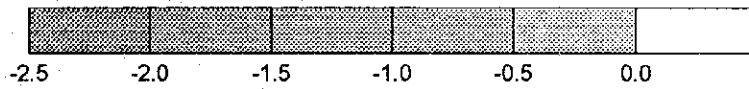
Faint, illegible text on the left edge of the page, possibly bleed-through from the reverse side.

Faint, illegible text on the right edge of the page, possibly bleed-through from the reverse side.





**RATE OF PIEZOMETRIC LEVEL CHANGE
IN PD AQUIFER FROM 1992 TO 1994 (m/year)**



• Location of production well
pumping from PD aquifer

Figure 6.2.3	RATE OF PIEZOMETRIC LEVEL CHANGE IN PD AQUIFER
THE STUDY ON MANAGEMENT OF GROUNDWATER AND LAND SUBSIDENCE IN THE BANGKOK METROPOLITAN AREA AND ITS VICINITY	
JAPAN INTERNATIONAL COOPERATION AGENCY (JICA)	KOKUSAI KOGYO CO., LTD.,

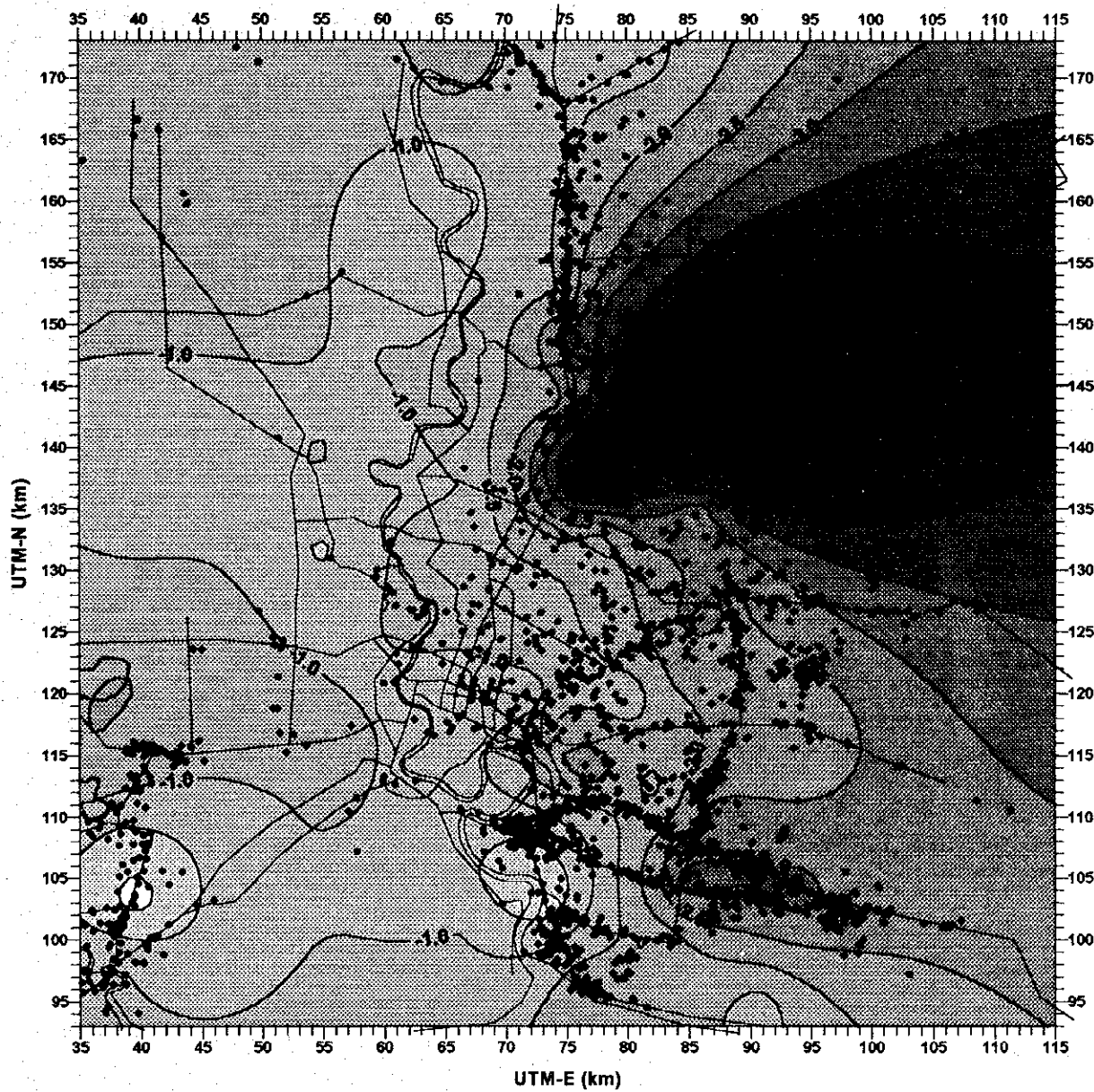
1. The first part of the document discusses the importance of maintaining accurate records of all transactions and activities. It emphasizes the need for transparency and accountability in financial reporting.

2. The second part of the document outlines the various methods and techniques used to collect and analyze data. It includes a detailed description of the experimental procedures and the tools used for data collection.

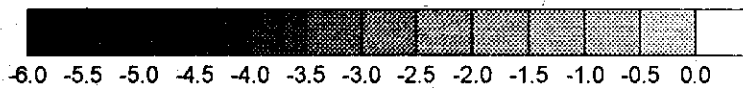
3. The third part of the document presents the results of the study. It includes a series of tables and graphs that illustrate the findings of the research. The data shows a clear trend in the relationship between the variables being studied.

4. The fourth part of the document discusses the implications of the findings. It highlights the potential applications of the research in various fields and the need for further investigation in this area.

5. The fifth part of the document concludes the study and provides a summary of the key findings. It also includes a list of references and a bibliography of the sources used in the research.



**RATE OF PIEZOMETRIC LEVEL CHANGE
IN NL AQUIFER FROM 1992 TO 1994 (m/year)**



• Location of production well
pumping from NL aquifer

Figure 6.2.5

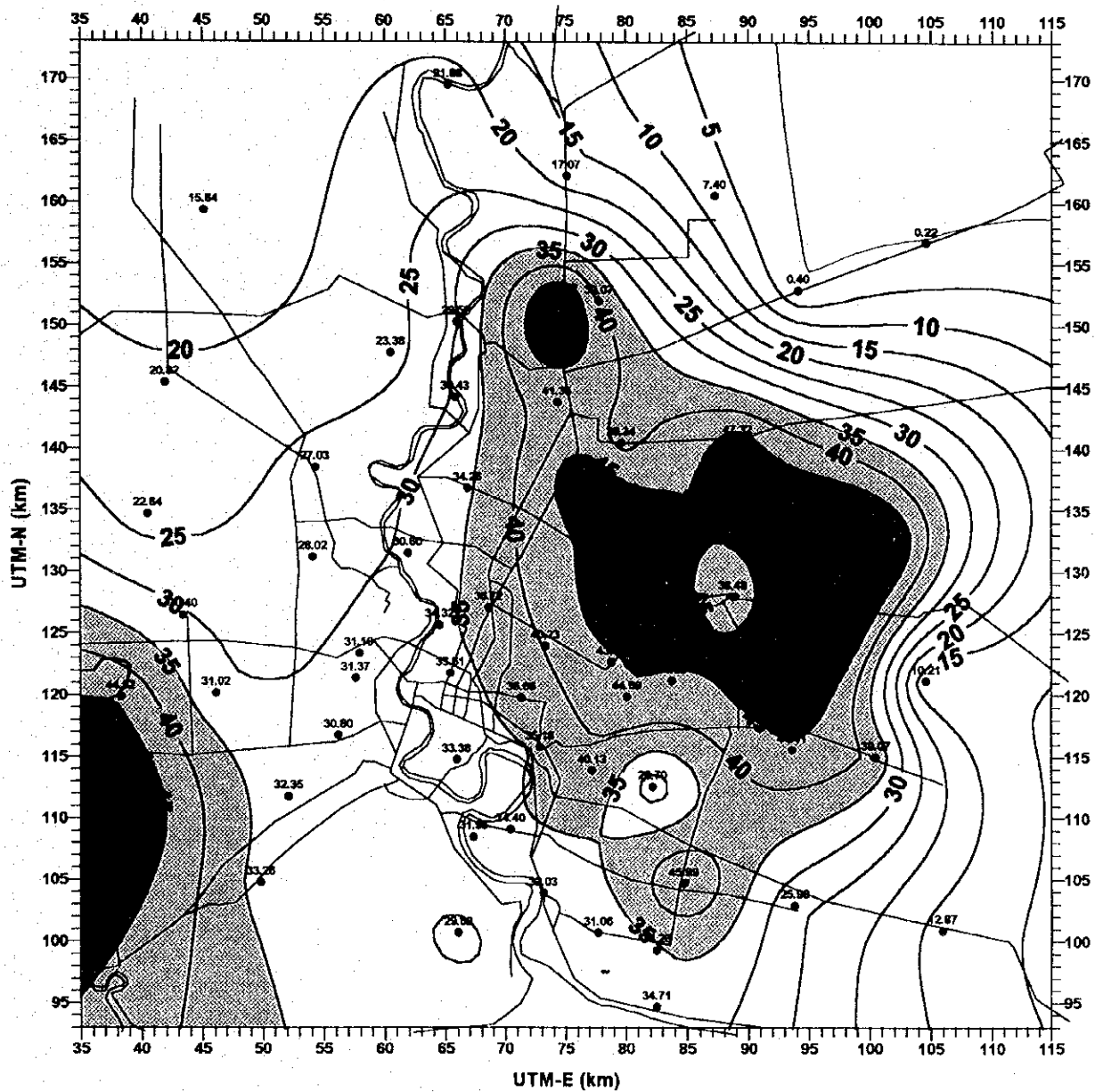
**RATE OF PIEZOMETRIC LEVEL CHANGE
IN NL AQUIFER**

**THE STUDY ON MANAGEMENT OF GROUNDWATER AND LAND SUBSIDENCE
IN THE BANGKOK METROPOLITAN AREA AND ITS VICINITY**

JAPAN INTERNATIONAL COOPERATION AGENCY (JICA)

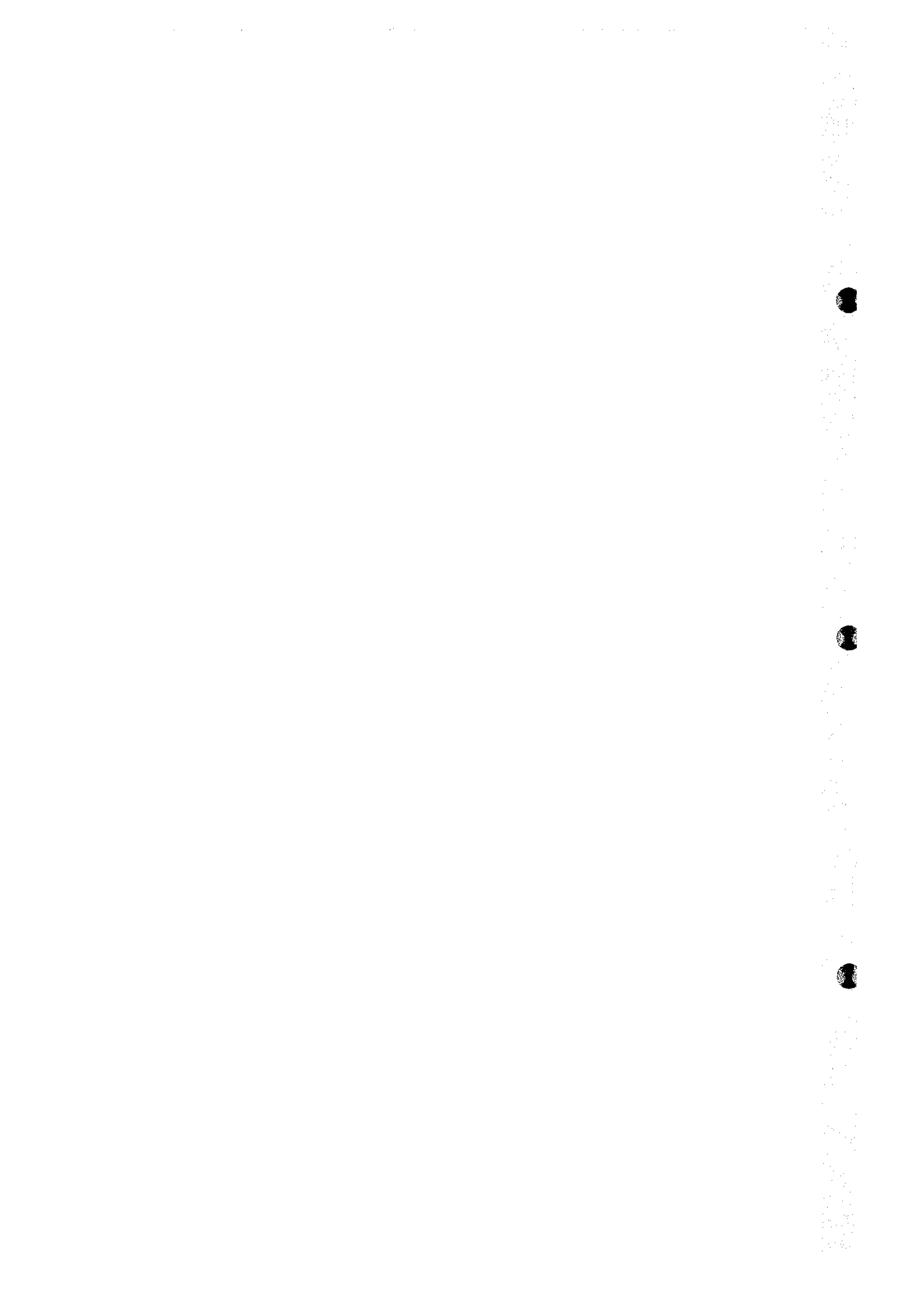
KOKUSAI KOGYO CO., LTD.

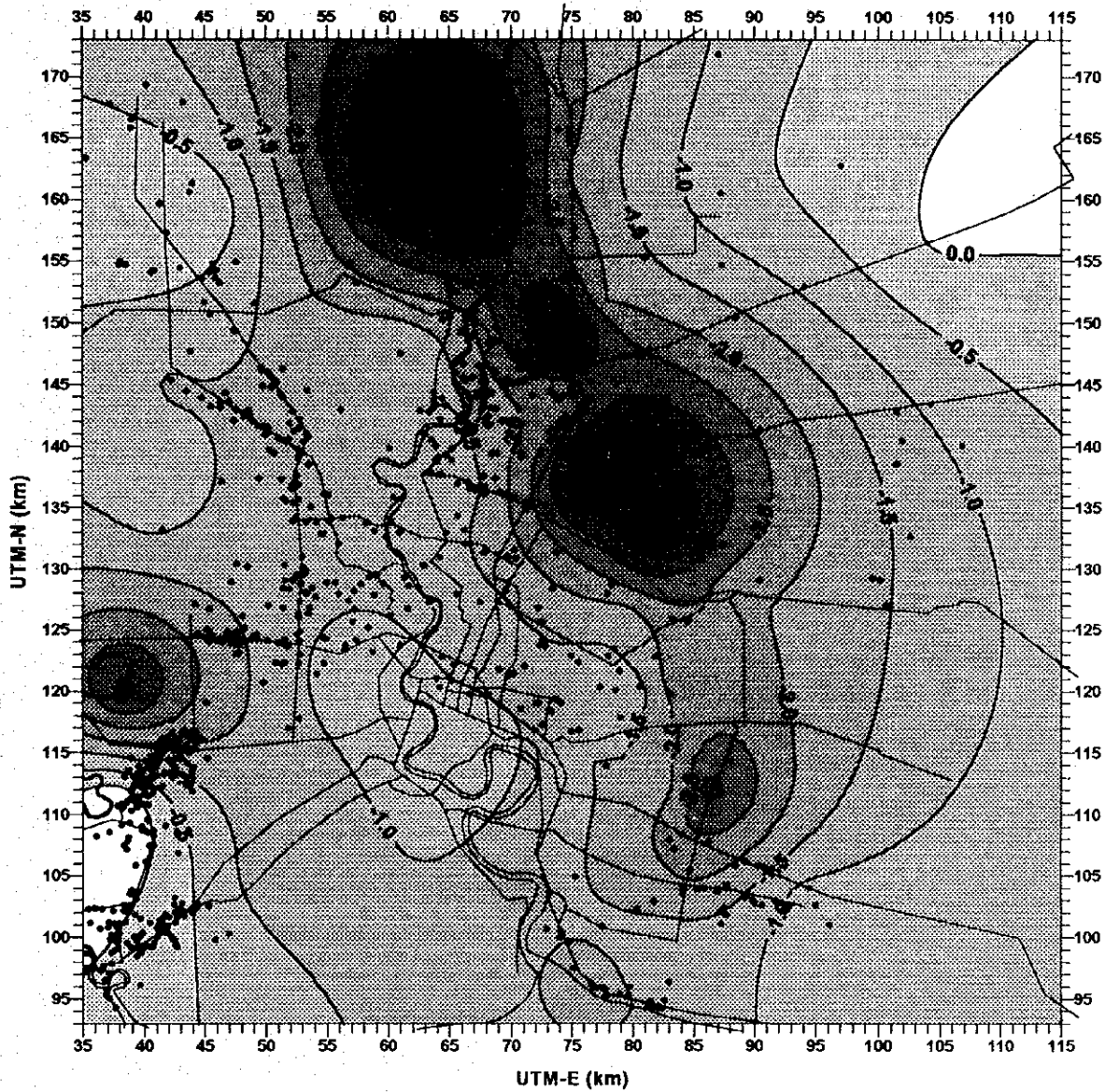




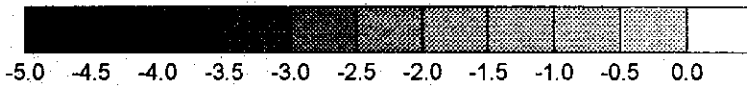
PIEZOMETRIC LEVEL (m below ground surface)

Figure 6.2.6	PIEZOMETRIC LEVELS OF NB AQUIFER IN MAY 1994
THE STUDY ON MANAGEMENT OF GROUNDWATER AND LAND SUBSIDENCE IN THE BANGKOK METROPOLITAN AREA AND ITS VICINITY	
JAPAN INTERNATIONAL COOPERATION AGENCY (JICA)	KOKUSAI KOGYO CO., LTD.





**RATE OF PIEZOMETRIC LEVEL CHANGE
IN NB AQUIFER FROM 1992 TO 1994 (m/year)**



• Location of production well
pumping from NB aquifer

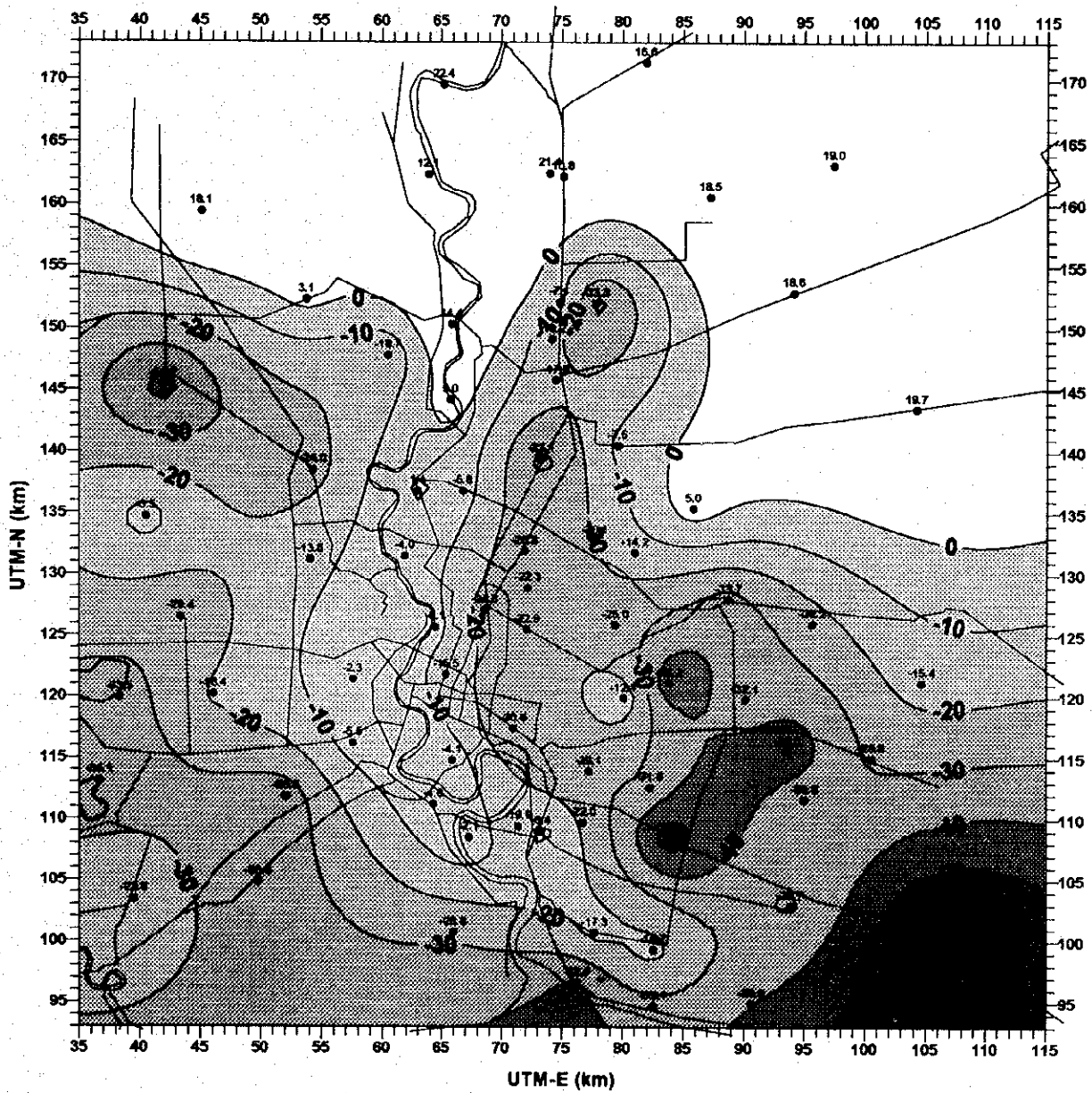
Figure 6.2.7

**RATE OF PIEZOMETRIC LEVEL CHANGE
IN NB AQUIFER**

**THE STUDY ON MANAGEMENT OF GROUNDWATER AND LAND SUBSIDENCE
IN THE BANGKOK METROPOLITAN AREA AND ITS VICINITY**

JAPAN INTERNATIONAL COOPERATION AGENCY (JICA)

KOKUSAI KOGYO CO., LTD:



LAND SUBSIDENCE (mm/year)

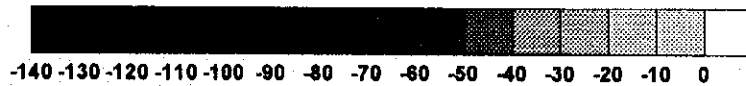


Figure 6.2.8	LAND SUBSIDENCE FROM 1992 TO 1993 MEASURED AT DMR 1m DEPTH BENCHMARKS
	THE STUDY ON MANAGEMENT OF GROUNDWATER AND LAND SUBSIDENCE IN THE BANGKOK METROPOLITAN AREA AND ITS VICINITY
JAPAN INTERNATIONAL COOPERATION AGENCY (JICA)	KOKUSAI KOGYO CO., LTD.

1
2
3
4
5
6
7
8
9
10
11
12
13
14
15
16
17
18
19
20
21
22
23
24
25
26
27
28
29
30
31
32
33
34
35
36
37
38
39
40
41
42
43
44
45
46
47
48
49
50
51
52
53
54
55
56
57
58
59
60
61
62
63
64
65
66
67
68
69
70
71
72
73
74
75
76
77
78
79
80
81
82
83
84
85
86
87
88
89
90
91
92
93
94
95
96
97
98
99
100
101
102
103
104
105
106
107
108
109
110
111
112
113
114
115
116
117
118
119
120
121
122
123
124
125
126
127
128
129
130
131
132
133
134
135
136
137
138
139
140
141
142
143
144
145
146
147
148
149
150
151
152
153
154
155
156
157
158
159
160
161
162
163
164
165
166
167
168
169
170
171
172
173
174
175
176
177
178
179
180
181
182
183
184
185
186
187
188
189
190
191
192
193
194
195
196
197
198
199
200
201
202
203
204
205
206
207
208
209
210
211
212
213
214
215
216
217
218
219
220
221
222
223
224
225
226
227
228
229
230
231
232
233
234
235
236
237
238
239
240
241
242
243
244
245
246
247
248
249
250
251
252
253
254
255
256
257
258
259
260
261
262
263
264
265
266
267
268
269
270
271
272
273
274
275
276
277
278
279
280
281
282
283
284
285
286
287
288
289
290
291
292
293
294
295
296
297
298
299
300
301
302
303
304
305
306
307
308
309
310
311
312
313
314
315
316
317
318
319
320
321
322
323
324
325
326
327
328
329
330
331
332
333
334
335
336
337
338
339
340
341
342
343
344
345
346
347
348
349
350
351
352
353
354
355
356
357
358
359
360
361
362
363
364
365
366
367
368
369
370
371
372
373
374
375
376
377
378
379
380
381
382
383
384
385
386
387
388
389
390
391
392
393
394
395
396
397
398
399
400
401
402
403
404
405
406
407
408
409
410
411
412
413
414
415
416
417
418
419
420
421
422
423
424
425
426
427
428
429
430
431
432
433
434
435
436
437
438
439
440
441
442
443
444
445
446
447
448
449
450
451
452
453
454
455
456
457
458
459
460
461
462
463
464
465
466
467
468
469
470
471
472
473
474
475
476
477
478
479
480
481
482
483
484
485
486
487
488
489
490
491
492
493
494
495
496
497
498
499
500
501
502
503
504
505
506
507
508
509
510
511
512
513
514
515
516
517
518
519
520
521
522
523
524
525
526
527
528
529
530
531
532
533
534
535
536
537
538
539
540
541
542
543
544
545
546
547
548
549
550
551
552
553
554
555
556
557
558
559
560
561
562
563
564
565
566
567
568
569
570
571
572
573
574
575
576
577
578
579
580
581
582
583
584
585
586
587
588
589
590
591
592
593
594
595
596
597
598
599
600
601
602
603
604
605
606
607
608
609
610
611
612
613
614
615
616
617
618
619
620
621
622
623
624
625
626
627
628
629
630
631
632
633
634
635
636
637
638
639
640
641
642
643
644
645
646
647
648
649
650
651
652
653
654
655
656
657
658
659
660
661
662
663
664
665
666
667
668
669
670
671
672
673
674
675
676
677
678
679
680
681
682
683
684
685
686
687
688
689
690
691
692
693
694
695
696
697
698
699
700
701
702
703
704
705
706
707
708
709
710
711
712
713
714
715
716
717
718
719
720
721
722
723
724
725
726
727
728
729
730
731
732
733
734
735
736
737
738
739
740
741
742
743
744
745
746
747
748
749
750
751
752
753
754
755
756
757
758
759
760
761
762
763
764
765
766
767
768
769
770
771
772
773
774
775
776
777
778
779
780
781
782
783
784
785
786
787
788
789
790
791
792
793
794
795
796
797
798
799
800
801
802
803
804
805
806
807
808
809
810
811
812
813
814
815
816
817
818
819
820
821
822
823
824
825
826
827
828
829
830
831
832
833
834
835
836
837
838
839
840
841
842
843
844
845
846
847
848
849
850
851
852
853
854
855
856
857
858
859
860
861
862
863
864
865
866
867
868
869
870
871
872
873
874
875
876
877
878
879
880
881
882
883
884
885
886
887
888
889
890
891
892
893
894
895
896
897
898
899
900
901
902
903
904
905
906
907
908
909
910
911
912
913
914
915
916
917
918
919
920
921
922
923
924
925
926
927
928
929
930
931
932
933
934
935
936
937
938
939
940
941
942
943
944
945
946
947
948
949
950
951
952
953
954
955
956
957
958
959
960
961
962
963
964
965
966
967
968
969
970
971
972
973
974
975
976
977
978
979
980
981
982
983
984
985
986
987
988
989
990
991
992
993
994
995
996
997
998
999
1000

6.3 Records of RTSD Benchmarks

The RTSD continues leveling survey at several types of benchmarks in and around the study area. The study team has selected only 1m depth benchmarks (CI-1 type and BMP type) to draw subsidence maps. Figure 6.3.1 shows the average rate of land subsidence from 1991 to 1993 measured at those 1m depth benchmarks. The areas having more than 30 mm/year of subsiding rate are widely distributed in Samut Prakan and eastern Bangkok. It is also found that some parts of Pathum Thani, central Bangkok, and Samut Sakhon show more than 30 mm/year.

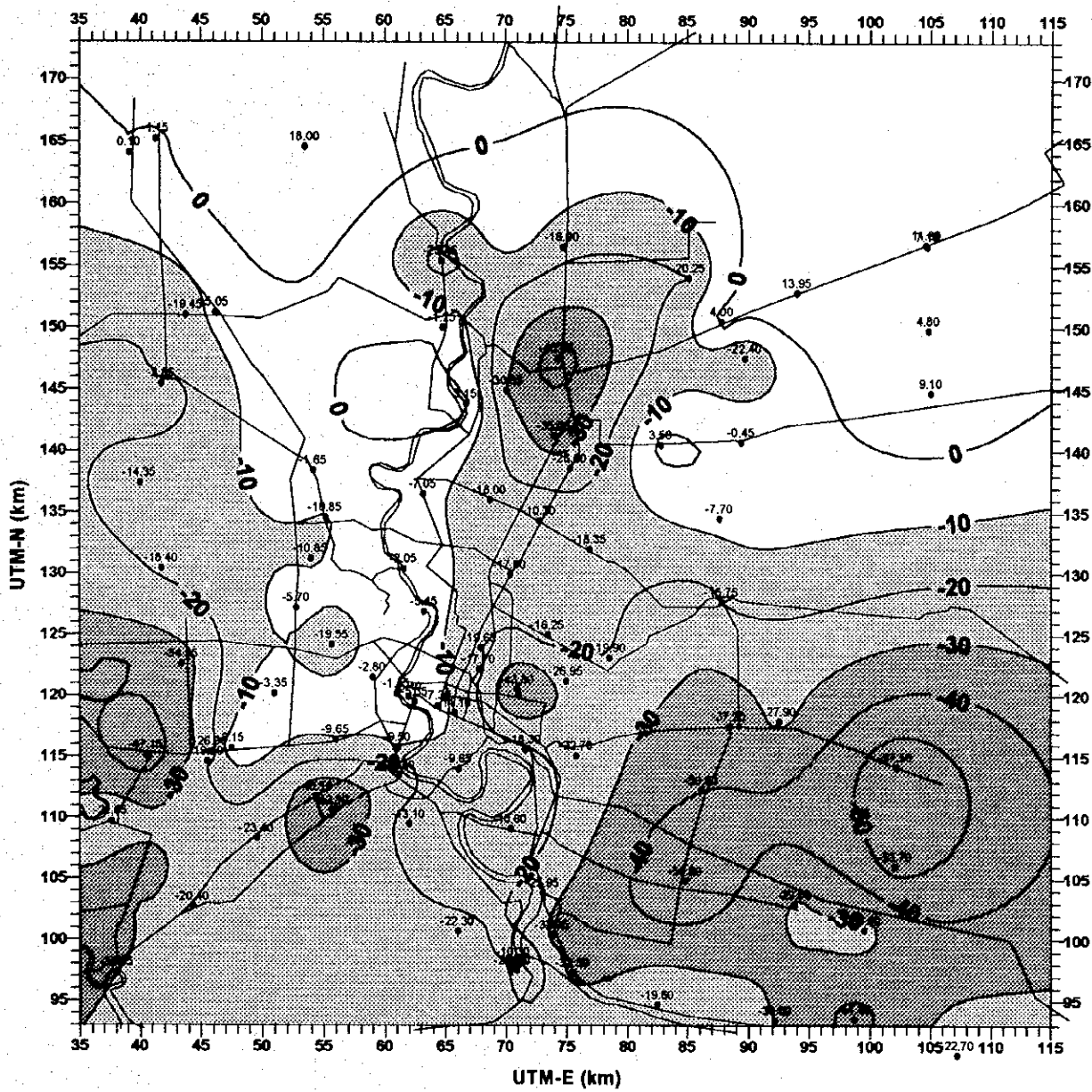
Figure 6.3.2 was prepared by compiling data from the DMR benchmarks and the RTSD benchmarks from 1992 to 1993. The map indicates significant land subsidence areas in Samut Prakan, eastern Bangkok, Pathum Thani, and Samut Sakhon, whereas the rate of subsidence is smaller along the Chao Phraya River.

The CI stations (= AIT stations) have different depths of benchmarks measured by the RTSD. The DMR has also started leveling survey at CI stations since 1991. Figure 6.3.3 shows land subsidence measured at AIT14 station, Wat Rajsathathum, Bangkok. This station is located near the center of significant land subsidence area. The subsidence value measured at CI-1 benchmark (1m depth) is 648.4 mm from 1980 to 1993. The lower graph shows land subsidence since 1986, indicating about 55% of compression occurs between the depths from 1.0m to 10.0m.

Similar graphs were prepared by using the data at AIT08 station, Chulalongkorn University, Bangkok (Figure 6.3.4). In this station, only CI-1 benchmark shows significant land subsidence since the start of measurement. The CI-4 benchmark shows rebound since 1981. The lower graph indicates that the contributions of 1.0m to 27.1m layer and 27.1m to 196.3m for land subsidence are 75% and 25%, respectively.

In Figure 6.3.5, the graphs at AIT25 station, AIT, Pathum Thani, show that the benchmarks of BM (depth = 19.0m), CI-2 (depth = 10.0m), and CI-4 (depth = 197.3m) indicate rebound since starting measurement. Even though the CI-1 benchmark shows rebound during periods from 1988 to 1990 and from 1992 to 1993.



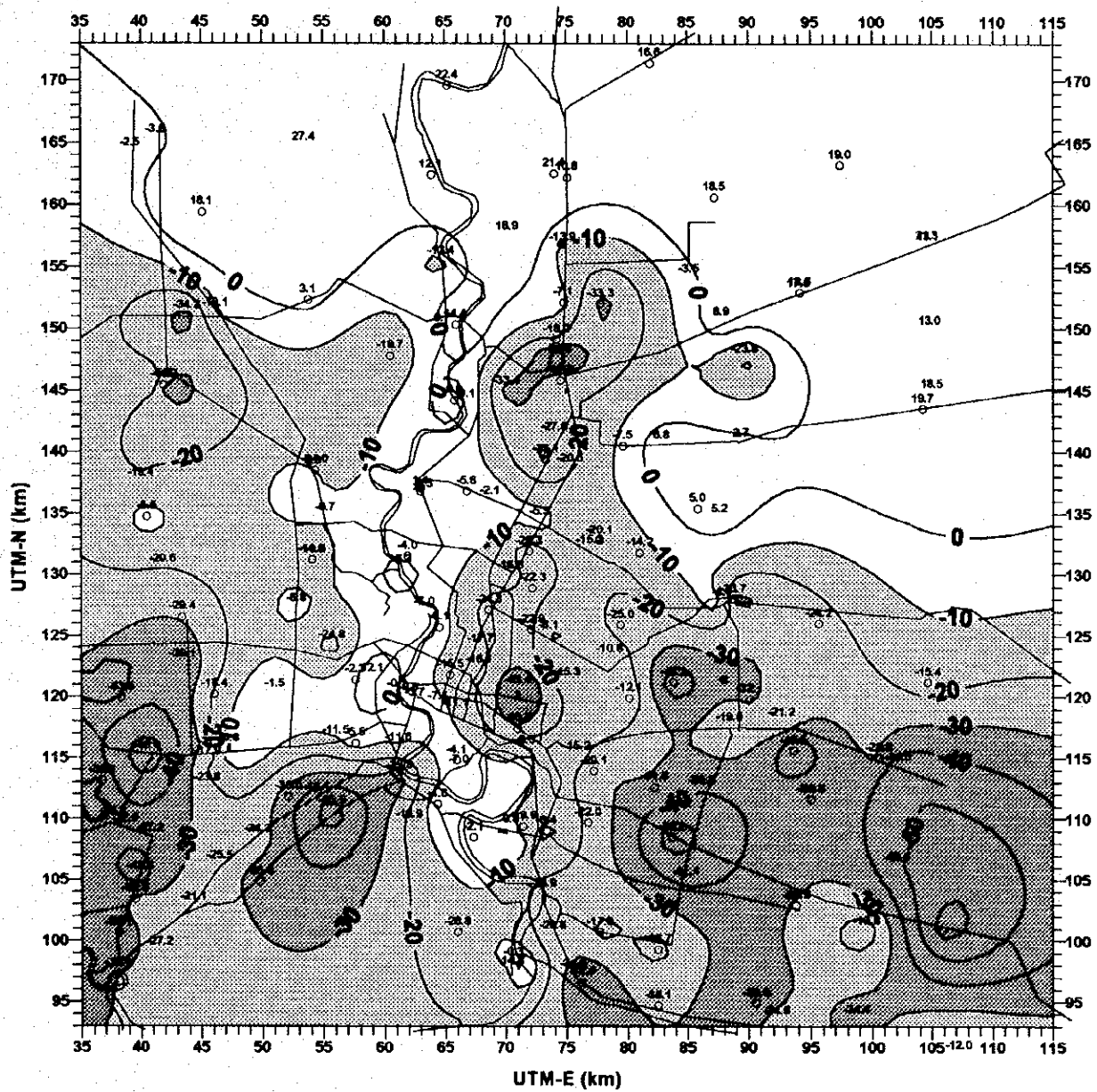


RATE OF LAND SUBSIDENCE FROM 1991 TO 1993 (mm/year)

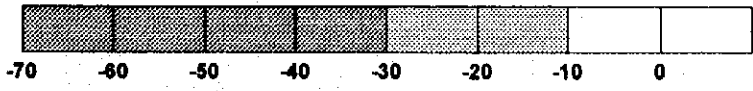
•^{-20.55} Location of RTSD 1m depth benchmark with rate of land subsidence from 1991 to 1993 (mm/year)

Figure 6.3.1	RATE OF LAND SUBSIDENCE AT RTSD 1m DEPTH BENCHMARKS
THE STUDY ON MANAGEMENT OF GROUNDWATER AND LAND SUBSIDENCE IN THE BANGKOK METROPOLITAN AREA AND ITS VICINITY	
JAPAN INTERNATIONAL COOPERATION AGENCY (JICA)	KOKUSAI KOGYO CO., LTD.





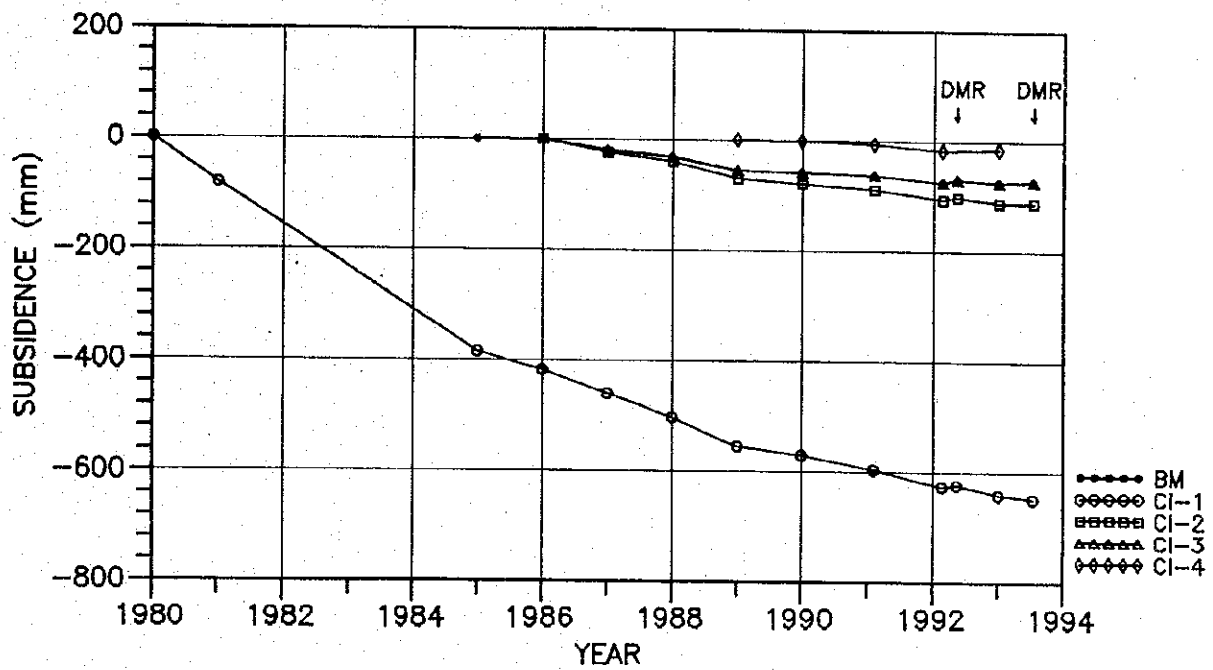
LAND SUBSIDENCE (mm/year)



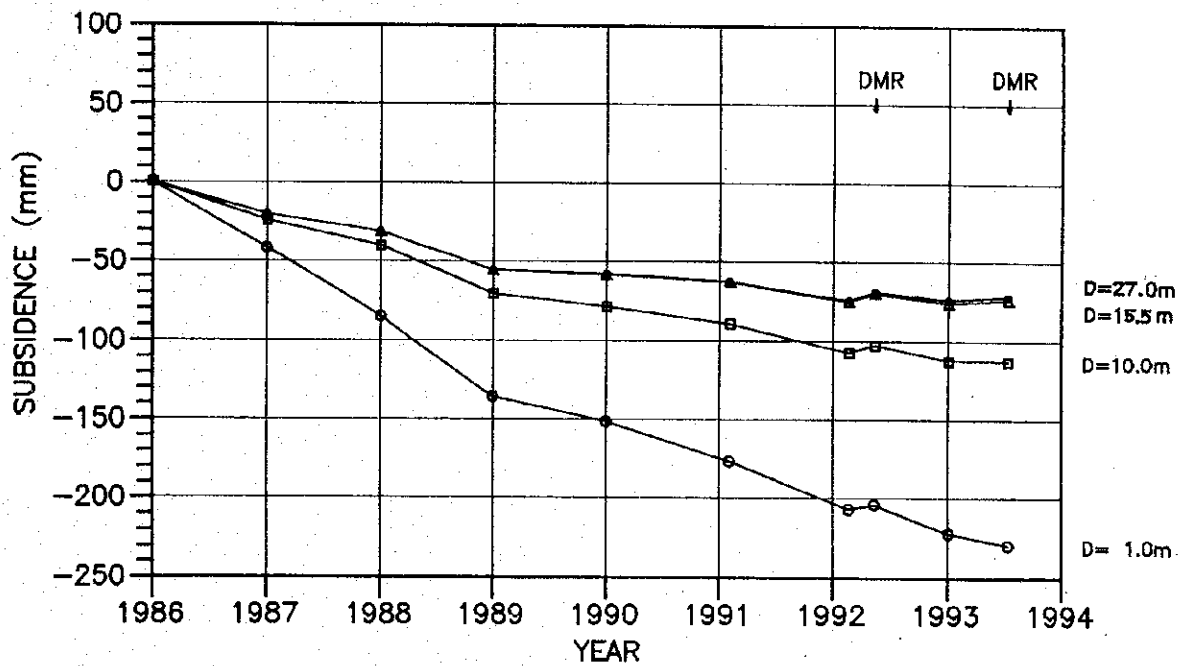
- DMR Benchmarks (1m depth)
- RTSD Benchmarks (1m depth)

Figure 6.3.2	LAND SUBSIDENCE FROM 1992 TO 1993 MEASURED AT 1m DEPTH BENCHMARKS
THE STUDY ON MANAGEMENT OF GROUNDWATER AND LAND SUBSIDENCE IN THE BANGKOK METROPOLITAN AREA AND ITS VICINITY	
JAPAN INTERNATIONAL COOPERATION AGENCY (JICA)	KOKUSAI KOGYO CO., LTD.





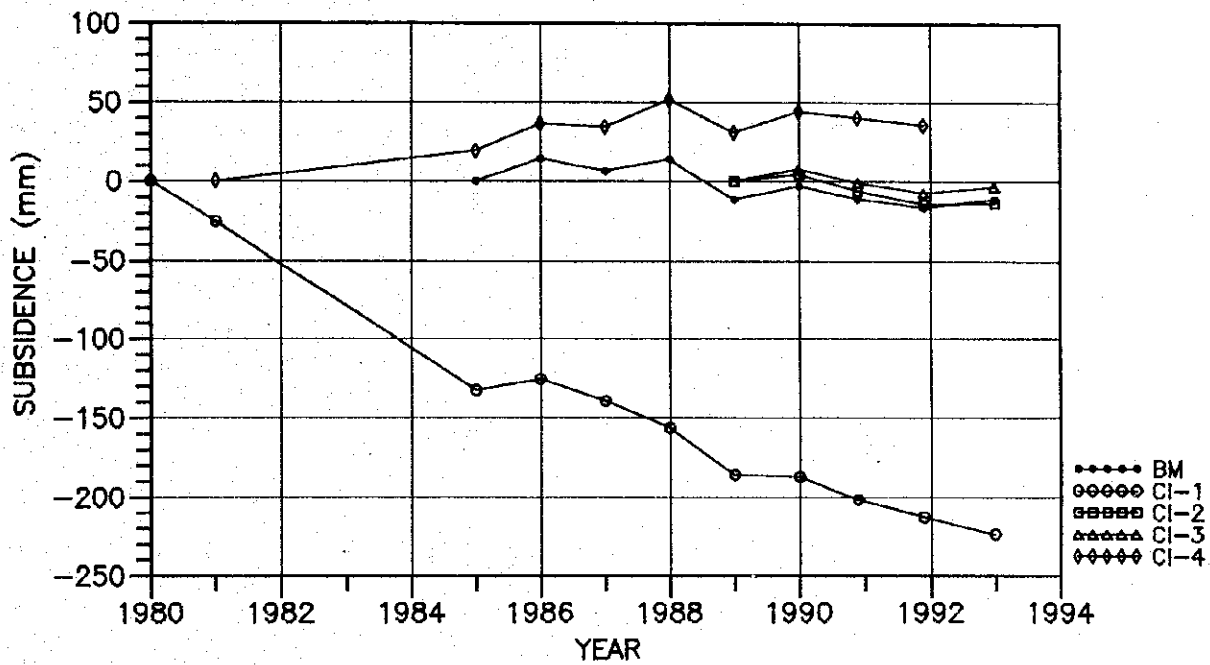
LAND SUBSIDENCE SINCE START OF MEASUREMENT



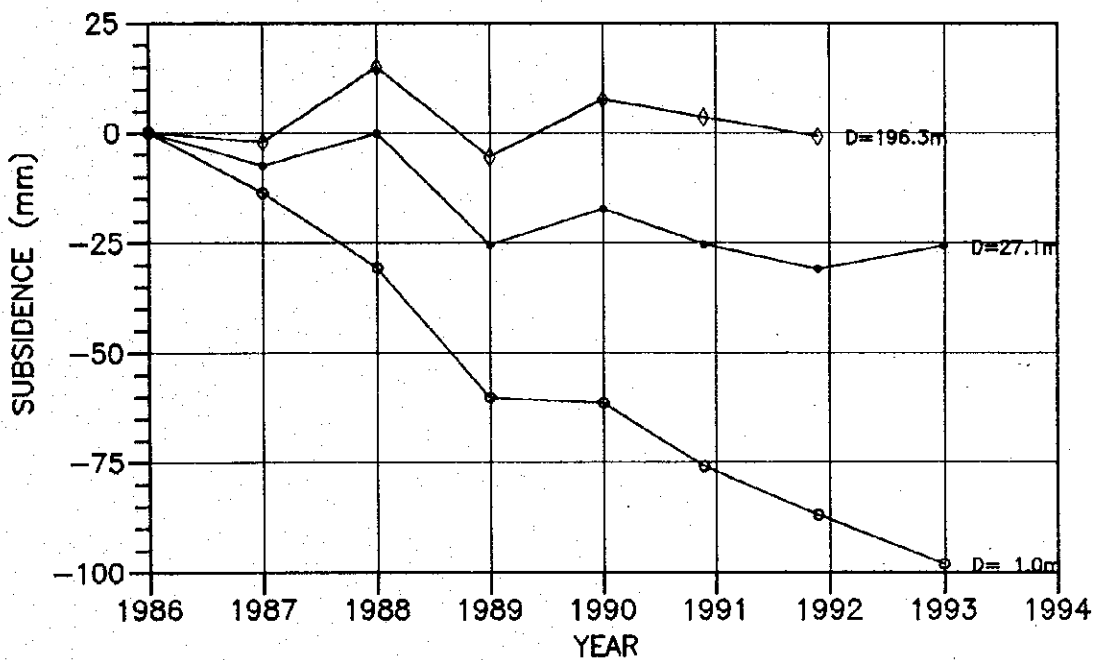
LAND SUBSIDENCE SINCE 1986

(DMR: Measured by DMR)

Figure 6.3.3	LAND SUBSIDENCE AT AIT14 STATION
THE STUDY ON MANAGEMENT OF GROUNDWATER AND LAND SUBSIDENCE IN THE BANGKOK METROPOLITAN AREA AND ITS VICINITY	
JAPAN INTERNATIONAL COOPERATION AGENCY (JICA)	KOKUSAI KOGYO CO., LTD.



LAND SUBSIDENCE SINCE START OF MEASUREMENT

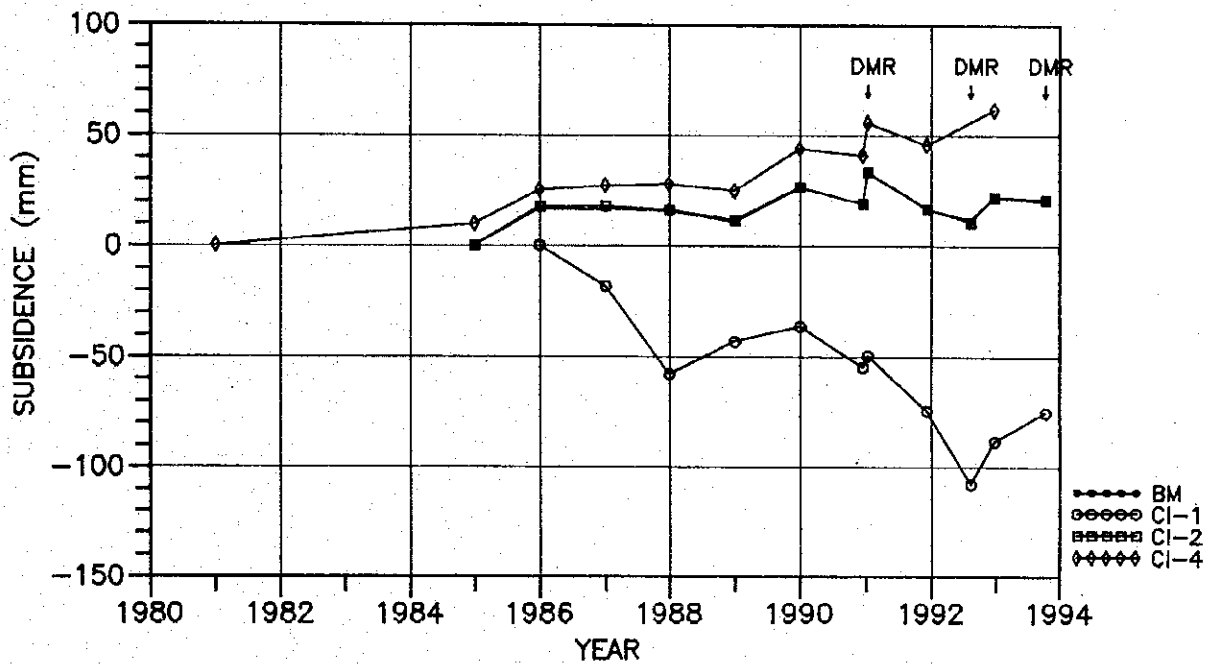


LAND SUBSIDENCE SINCE 1986

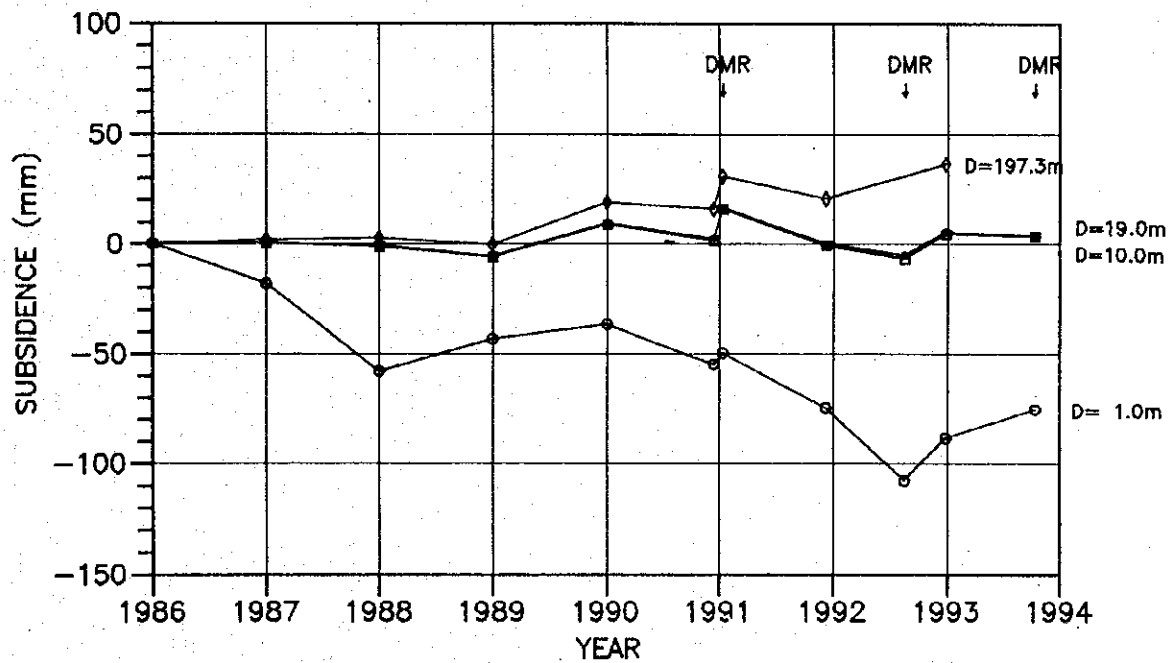
(DMR: Measured by DMR)

Figure 6.3.4	LAND SUBSIDENCE AT ATOB STATION
THE STUDY ON MANAGEMENT OF GROUNDWATER AND LAND SUBSIDENCE IN THE BANGKOK METROPOLITAN AREA AND ITS VICINITY	
JAPAN INTERNATIONAL COOPERATION AGENCY (JICA)	KOKUSAI KOGYO CO., LTD.





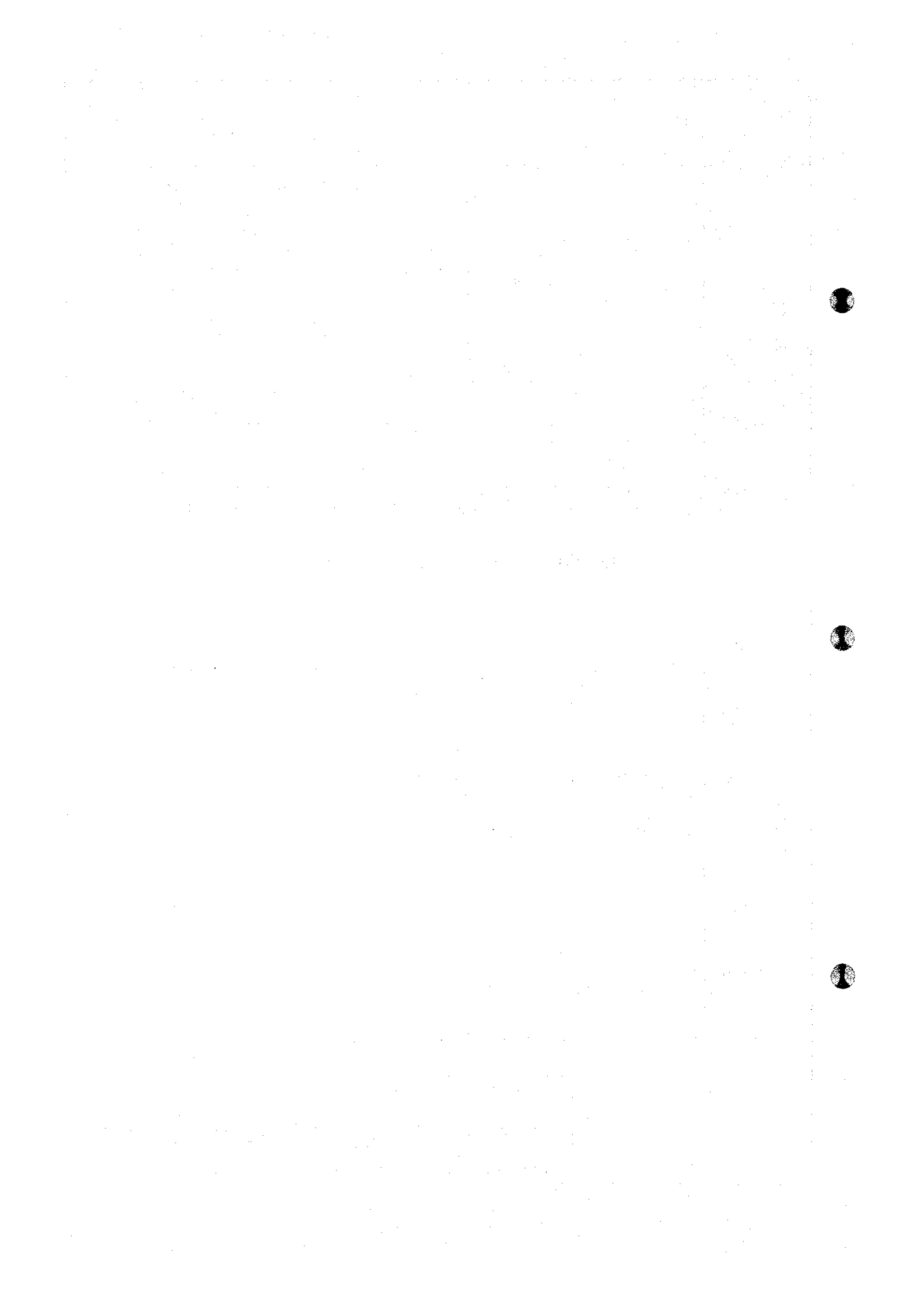
LAND SUBSIDENCE SINCE START OF MEASUREMENT



LAND SUBSIDENCE SINCE 1986

(DMR: Measured by DMR)

Figure 6.3.5	LAND SUBSIDENCE AT AIT25 STATION
THE STUDY ON MANAGEMENT OF GROUNDWATER AND LAND SUBSIDENCE IN THE BANGKOK METROPOLITAN AREA AND ITS VICINITY	
JAPAN INTERNATIONAL COOPERATION AGENCY (JICA)	KOKUSAI KOGYO CO., LTD.



CONTENTS

CHAPTER 7 COMPUTER MODELING AND PREDICTIONS	7-1
7.1 General	7-1
7.2 3-D Groundwater Flow and Land Subsidence Model	7-3
7.2.1 Model Concept	7-3
7.2.2 Groudwater Flow Equation	7-3
7.2.3 Land Subsidence Equation	7-4
7.2.4 Required Input Data and Output Data	7-5
7.2.5 Model Assumptions	7-6
7.2.6 Model Grid	7-6
7.2.7 Boundary Conditions	7-7
7.2.8 Hydrogeologic Parameters	7-8
7.2.9 Model Calibration	7-13
7.2.10 Predictions	7-17
7.3 Vertical 2-D Groundwater Flow and Land Subsidence Model	7-120
7.3.1 Model Concept	7-120
7.3.2 Groudwater Flow Equation	7-120
7.3.3 Land Subsidence Equation	7-121
7.3.4 Required Input Data and Output Data	7-121
7.3.5 Model Assumptions	7-123
7.3.6 Model Grid	7-123
7.3.7 Boundary Conditions	7-123
7.3.8 Hydrogeologic Parameters	7-124
7.3.9 Model Calibration	7-125
7.3.10 Predictions	7-127
7.4 Vertical 2-D Solute Transport Model	7-151
7.4.1 Model Concept	7-151
7.4.2 Flow Equation of Variable Density Fluid	7-152
7.4.3 Solute Transport Equation	7-152
7.4.4 Required Input Data and Output Data	7-152
7.4.5 Model Assumptions	7-154
7.4.6 Model Grid	7-154
7.4.7 Boundary Conditions	7-155
7.4.8 Hydrogeologic Parameters	7-155
7.4.9 Model Calibration	7-157
7.4.10 Predictions	7-159

LIST OF TABLES

7.2.1	AVERAGE VALUES OF QUARTERLY GROUNDWATER PUMPAGE COEFFICIENTS (QGPC)	7-14
7.2.2	IDENTIFIED VALUES OF m_v AND m_v/m_v'	7-17
7.2.3	SUMMARY OF FUTURE PUMPAGE SCENARIO	7-22

LIST OF FIGURES

7.1.1	FLOW OF GROUNDWATER MODELING	7-2
7.2.1	GRID FOR 3-D MODFLOW MODEL	7-23
7.2.2	STRUCTURE OF 3-D MODEL	7-24
7.2.3	CONCEPT OF 3-D MODEL APPLIED TO BANGKOK AQUIFER SYSTEM	7-25
7.2.4	BOUNDARIES OF AQUIFER UNITS (BC TO NB) FOR MODFLOW 3-D MODEL	7-26
7.2.5	BOUNDARIES OF AQUIFER UNITS (NB TO PN) FOR MODFLOW 3-D MODEL	7-27
7.2.6	ELEVATION OF GROUND SURFACE	7-28
7.2.7	ISOPACH MAP OF BANGKOK SOFT CLAY	7-29
7.2.8	DEPTH TO THE BOTTOM OF BK AQUIFER	7-30
7.2.9	DEPTH TO THE BOTTOM OF PD AQUIFER	7-31
7.2.10	DEPTH TO THE BOTTOM OF NL AQUIFER	7-32
7.2.11	DEPTH TO THE BOTTOM OF NB AQUIFER	7-33
7.2.12	DEPTH TO THE BOTTOM OF SK AQUIFER	7-34
7.2.13	DEPTH TO THE BOTTOM OF PT AQUIFER	7-35
7.2.14	DEPTH TO THE BOTTOM OF TB AQUIFER	7-36
7.2.15	DISTRIBUTION OF SPECIFIC CAPACITY VALUES OBTAINED FROM PRODUCTION WELLS DATA	7-37
7.2.16	DISTRIBUTION OF SPECIFIC CAPACITY IN BK AQUIFER	7-38
7.2.17	DISTRIBUTION OF SPECIFIC CAPACITY IN PD AQUIFER	7-39
7.2.18	DISTRIBUTION OF SPECIFIC CAPACITY IN NL AQUIFER	7-40
7.2.19	DISTRIBUTION OF SPECIFIC CAPACITY IN NB AQUIFER	7-41
7.2.20	DISTRIBUTION OF SPECIFIC CAPACITY IN SK AQUIFER	7-42
7.2.21	DISTRIBUTION OF SPECIFIC CAPACITY IN PT AQUIFER	7-43
7.2.22	DISTRIBUTION OF SPECIFIC CAPACITY IN TB AQUIFER	7-44
7.2.23	DISTRIBUTION OF SPECIFIC CAPACITY IN PN AQUIFER	7-45
7.2.24	DISTRIBUTION OF PERMEABILITY VALUES ESTIMATE FROM PRODUCTION WELLS DATA	7-46
7.2.25	ESTIMATED PERMEABILITY OF BK AQUIFER	7-47
7.2.26	ESTIMATED PERMEABILITY OF PD AQUIFER	7-48
7.2.27	ESTIMATED PERMEABILITY OF NL AQUIFER	7-49
7.2.28	ESTIMATED PERMEABILITY OF NB AQUIFER	7-50
7.2.29	ESTIMATED PERMEABILITY OF SK AQUIFER	7-51
7.2.30	ESTIMATED PERMEABILITY OF PT AQUIFER	7-52
7.2.31	ESTIMATED PERMEABILITY OF TB AQUIFER	7-53
7.2.32	ESTIMATED PERMEABILITY OF PN AQUIFER	7-54

7.2.33 ISOPACH MAP OF BK AQUIFER	7-55
7.2.34 ISOPACH MAP OF PD AQUIFER	7-56
7.2.35 ISOPACH MAP OF NL AQUIFER	7-57
7.2.36 ISOPACH MAP OF NB AQUIFER	7-58
7.2.37 ISOPACH MAP OF SK AQUIFER	7-59
7.2.38 ISOPACH MAP OF PT AQUIFER	7-60
7.2.39 ISOPACH MAP OF TB AQUIFER	7-61
7.2.40 CLAY CONTENT OF BK AQUIFER	7-62
7.2.41 CLAY CONTENT OF PD AQUIFER	7-63
7.2.42 CLAY CONTENT OF NL AQUIFER	7-64
7.2.43 CLAY CONTENT OF NB AQUIFER	7-65
7.2.44 CLAY CONTENT OF SK AQUIFER	7-66
7.2.45 CLAY CONTENT OF PT AQUIFER	7-67
7.2.46 CLAY CONTENT OF TB AQUIFER	7-68
7.2.47 ESTIMATED TRANSMISSIVITY OF BK AQUIFER	7-69
7.2.48 ESTIMATED TRANSMISSIVITY OF PD AQUIFER	7-70
7.2.49 ESTIMATED TRANSMISSIVITY OF NL AQUIFER	7-71
7.2.50 ESTIMATED TRANSMISSIVITY OF NB AQUIFER	7-72
7.2.51 ESTIMATED TRANSMISSIVITY OF SK AQUIFER	7-73
7.2.52 ESTIMATED TRANSMISSIVITY OF PT AQUIFER	7-74
7.2.53 ESTIMATED TRANSMISSIVITY OF TB AQUIFER	7-75
7.2.54 ESTIMATED TRANSMISSIVITY OF PN AQUIFER	7-76
7.2.55 DISTRIBUTION OF CLAY PERMEABILITIES ESTIMATE FROM CONSOLIDATION TESTS	7-77
7.2.56 DISTRIBUTION OF VOLUME COMPRESSIBILITY	7-78
7.2.57 RELATION BETWEEN DEPTH AND VOLUME COMPRESSIBILITY (m_v) AT CI-STATIONS	7-79
7.2.58 CHANGES IN VOLUME COMPRESSIBILITY WITH GROUND- WATER PRESSURE AT SITE-A	7-80
7.2.59 HISTORICAL GROUNDWATER PUMPAGE IN THE STUDY AREA BY AQUIFER UNIT	7-81
7.2.60 DISTRIBUTION OF GROUNDWATER PUMPAGE FROM PD AQUIFER IN 1983	7-82
7.2.61 DISTRIBUTION OF GROUNDWATER PUMPAGE FROM PD AQUIFER IN 1992	7-83
7.2.62 DISTRIBUTION OF GROUNDWATER PUMPAGE FROM NL AQUIFER IN 1983	7-84
7.2.63 DISTRIBUTION OF GROUNDWATER PUMPAGE FROM NL AQUIFER IN 1992	7-85
7.2.64 DISTRIBUTION OF GROUNDWATER PUMPAGE FROM NB AQUIFER IN 1983	7-86
7.2.65 DISTRIBUTION OF GROUNDWATER PUMPAGE FROM NB AQUIFER IN 1992	7-87
7.2.66 COMPARISON OF SIMULATED HEADS BY 3-D MODEL WITH ACTUAL HEADS	7-88
7.2.67 SIMULATED AND ACTUAL PIEZOMETRIC LEVELS OF PD AQUIFER AT THE END OF 1992	7-89
7.2.68 SIMULATED AND ACTUAL PIEZOMETRIC LEVELS OF NL AQUIFER AT THE END OF 1992	7-90

7.2.69	SIMULATED AND ACTUAL PIEZOMETRIC LEVELS OF NB AQUIFER AT THE END OF 1992	7-91
7.2.70	SIMULATED LAND SUBSIDENCE FROM 1983 TO 1992	7-92
7.2.71	SIMULATED PIEZOMETRIC HEADS AT JICA MONITORING STATIONS (SCENARIO 1)	7-93
7.2.72	SIMULATED LAND SUBSIDENCE (FUTURE SCENARIO 1)	7-94
7.2.73	SIMULATED LAND SUBSIDENCE BY FUTURE SCENARIO 1	7-95
7.2.74	SIMULATED PIEZOMETRIC HEADS AT JICA MONITORING STATIONS (SCENARIO 2)	7-96
7.2.75	SIMULATED LAND SUBSIDENCE (FUTURE SCENARIO 2)	7-97
7.2.76	SIMULATED LAND SUBSIDENCE BY FUTURE SCENARIO 2	7-98
7.2.77	SIMULATED PIEZOMETRIC HEADS AT JICA MONITORING STATIONS (SCENARIO 3)	7-99
7.2.78	SIMULATED LAND SUBSIDENCE (FUTURE SCENARIO 3)	7-100
7.2.79	SIMULATED LAND SUBSIDENCE BY FUTURE SCENARIO 3	7-101
7.2.80	SIMULATED PIEZOMETRIC HEADS AT JICA MONITORING STATIONS (SCENARIO 4)	7-102
7.2.81	SIMULATED LAND SUBSIDENCE (FUTURE SCENARIO 4)	7-103
7.2.82	SIMULATED LAND SUBSIDENCE BY FUTURE SCENARIO 4	7-104
7.2.83	SIMULATED PIEZOMETRIC HEADS AT JICA MONITORING STATIONS (SCENARIO 5A)	7-105
7.2.84	SIMULATED LAND SUBSIDENCE (FUTURE SCENARIO 5A)	7-106
7.2.85	SIMULATED LAND SUBSIDENCE BY FUTURE SCENARIO 5A	7-107
7.2.86	SIMULATED PIEZOMETRIC HEADS AT JICA MONITORING STATIONS (SCENARIO 5B)	7-108
7.2.87	SIMULATED LAND SUBSIDENCE (FUTURE SCENARIO 5B)	7-109
7.2.88	SIMULATED LAND SUBSIDENCE BY FUTURE SCENARIO 5B	7-110
7.2.89	SIMULATED PIEZOMETRIC HEADS AT JICA MONITORING STATIONS (SCENARIO 5C)	7-111
7.2.90	SIMULATED LAND SUBSIDENCE (FUTURE SCENARIO 5C)	7-112
7.2.91	SIMULATED LAND SUBSIDENCE BY FUTURE SCENARIO 5C	7-113
7.2.92	SIMULATED PIEZOMETRIC HEADS AT JICA MONITORING STATIONS (SCENARIO 6)	7-114
7.2.93	SIMULATED LAND SUBSIDENCE (FUTURE SCENARIO 6)	7-115
7.2.94	SIMULATED LAND SUBSIDENCE BY FUTURE SCENARIO 6	7-116
7.2.95	SIMULATED PIEZOMETRIC HEADS AT JICA MONITORING STATIONS (SCENARIO 7)	7-117
7.2.96	SIMULATED LAND SUBSIDENCE (FUTURE SCENARIO 7)	7-118
7.2.97	SIMULATED LAND SUBSIDENCE BY FUTURE SCENARIO 7	7-119
7.3.1	LOCATION OF VERTICAL 2-D MODELS	7-128
7.3.2	LOCATION OF VERTICAL 2-D LAND SUBSIDENCE MODEL	7-129
7.3.3	VERTICAL 2-D LAND SUBSIDENCE MODEL GRID	7-130
7.3.4	HYDROGEOLOGIC UNIT AND FACIES ALLOCATION FOR VERTICAL 2-D LAND SUBSIDENCE MODEL	7-131
7.3.5	$e - \log P$ CURVES OF CLAYEY SOILS (DEPTH = 0.0m to 5.0m)	7-132
7.3.6	$e - \log P$ CURVES OF CLAYEY SOILS (DEPTH = 5.0m to 10.0m)	7-133
7.3.7	$e - \log P$ CURVES OF CLAYEY SOILS (DEPTH = 10.0m to 15.0m)	7-134
7.3.8	$e - \log P$ CURVES OF CLAYEY SOILS (DEPTH = 15.0m to 20.0m)	7-135

7.3.9	log m_v - log P_{av} CURVES OF CLAYEY SOILS (DEPTH = 0.0m to 5.0m)	7-136
7.3.10	log m_v - log P_{av} CURVES OF CLAYEY SOILS (DEPTH = 5.0m to 10.0m)	7-137
7.3.11	log m_v - log P_{av} CURVES OF CLAYEY SOILS (DEPTH = 10.0m to 15.0m)	7-138
7.3.12	log m_v - log P_{av} CURVES OF CLAYEY SOILS (DEPTH = 15.0m to 20.0m)	7-139
7.3.13	DISTRIBUTION OF GROUNDWATER PUMPAGE IN 1992 FOR VERTICAL 2-D LAND SUBSIDENCE MODEL	7-140
7.3.14	SIMULATED PIEZOMETRIC HEADS IN 1992 BY VERTICAL 2-D LAND SUBSIDENCE MODEL	7-141
7.3.15	SIMULATED COMPRESSION FROM 1983 TO 1992 BY VERTICAL 2-D LAND SUBSIDENCE MODEL	7-142
7.3.16	RESULTS OF LAND SUBSIDENCE SIMULATION BY VERTICAL 2-D MODEL	7-143
7.3.17	SIMULATED PIEZOMETRIC HEADS BY SCENARIO 1	7-145
7.3.18	SIMULATED COMPRESSION FROM 1993 TO 2017 BY SCENARIO 1	7-146
7.3.19	SIMULATED LAND SUBSIDENCE BY SCENARIO 1	7-147
7.3.20	SIMULATED PIEZOMETRIC HEADS BY SCENARIO 7	7-148
7.3.21	SIMULATED COMPRESSION FROM 1993 TO 2017 BY SCENARIO 7	7-149
7.3.22	SIMULATED LAND SUBSIDENCE BY SCENARIO 7	7-150
7.4.1	LOCATION OF VERTICAL 2-D SOLUTE TRANSPORT MODEL	7-161
7.4.2	VERTICAL 2-D SOLUTE TRANSPORT MODEL GRID	7-162
7.4.3	HYDROGEOLOGIC UNIT AND FACIES ALLOCATION FOR VERTICAL 2-D SOLUTE TRANSPORT MODEL	7-163
7.4.4	DISTRIBUTION OF GROUNDWATER PUMPAGE IN 1992 FOR VERTICAL 2-D SOLUTE TRANSPORT MODEL	7-164
7.4.5	SIMULATED PIEZOMETRIC HEADS IN 1992 BY VERTICAL 2-D SOLUTE TRANSPORT MODEL	7-165
7.4.6	SIMULATED STEADY-STATE CHLORIDE CONCENTRATION BY MOCDENSE	7-166
7.4.7	SIMULATED CHLORIDE CONCENTRATION IN 1992 BY MOCDENSE AND MT3D	7-167
7.4.8	SIMULATED CHLORIDE CONCENTRATION IN 1992 BY MT3D (CASE-1)	7-168
7.4.9	SIMULATED CHLORIDE CONCENTRATION IN 1992 BY MT3D (CASE-2)	7-169
7.4.10	SIMULATED PIEZOMETRIC HEADS BY SCENARIO 1	7-170
7.4.11	SIMULATED CHLORIDE CONCENTRATION BY SCENARIO 1	7-171
7.4.12	SIMULATED PIEZOMETRIC HEADS BY SCENARIO 1	7-172
7.4.13	SIMULATED CHLORIDE CONCENTRATION BY SCENARIO 1	7-173

CHAPTER 7 COMPUTER MODELING AND PREDICTIONS

7.1 General

The construction of the groundwater flow model, land subsidence model, and solute transport model for the Bangkok aquifer system was based on various kinds of the hydrogeological analyses done by the Study Team. This modeling activity is undertaken to predict future piezometric level and land subsidence, and specifically to:

- (1) Describe the hydrogeologic conditions that led to heavy decline of piezometric level, land subsidence, and saline water intrusion; and
- (2) To estimate the behavior of groundwater and land subsidence resulting from future groundwater use plans or regulations.

Because groundwater is essentially an invisible resource, studies of groundwater movement under natural and artificial conditions require modeling techniques. Several types of models have been developed and used for this purpose. In recent years, digital computer models have gained wider acceptance as they foster more efficient groundwater resources management. These tools have considerable capability to aid decision-making in relation to the various uses of both actual and potential groundwater systems.

Digital groundwater models may be further subdivided into flow models and solute transport models. Flow models consist of a set of differential equations that are known to govern the flow of groundwater. Solute transport models are based on a flow component and are coupled with the solute transport equations. They are used to predict the movement and concentration in the aquifers of various pollutants including saline water intrusion in coastal areas.

Land subsidence models use the consolidation theory of soils. There are several approaches to compute soil consolidation in the field of soil engineering. For the land subsidence simulation, changes in groundwater pressure obtained from piezometric level are important besides the consolidation parameters.

Figure 7.1.1 shows the flow of groundwater modeling. After defining the purpose, each model was established based on accurate hydrogeological investigations and analyses. Appropriate boundary conditions and geohydrologic parameters were assigned to each model. Initial calibration for each model was carried out by steady-state simulation to understand the model behavior. The assigned boundary conditions and the input parameters were checked and/or modified by comparing computed piezometric heads with the actual piezometric heads.

The reliability of prediction using a groundwater model or a land subsidence model depends on how well the model approximates the field situation. As natural aquifer systems are inherently complex and uncertain, construction of the model always requires the making of assumptions and simplifications. It is very important to keep this awareness about the model, even though sophisticated numerical techniques and high-speed computers have already been developed.

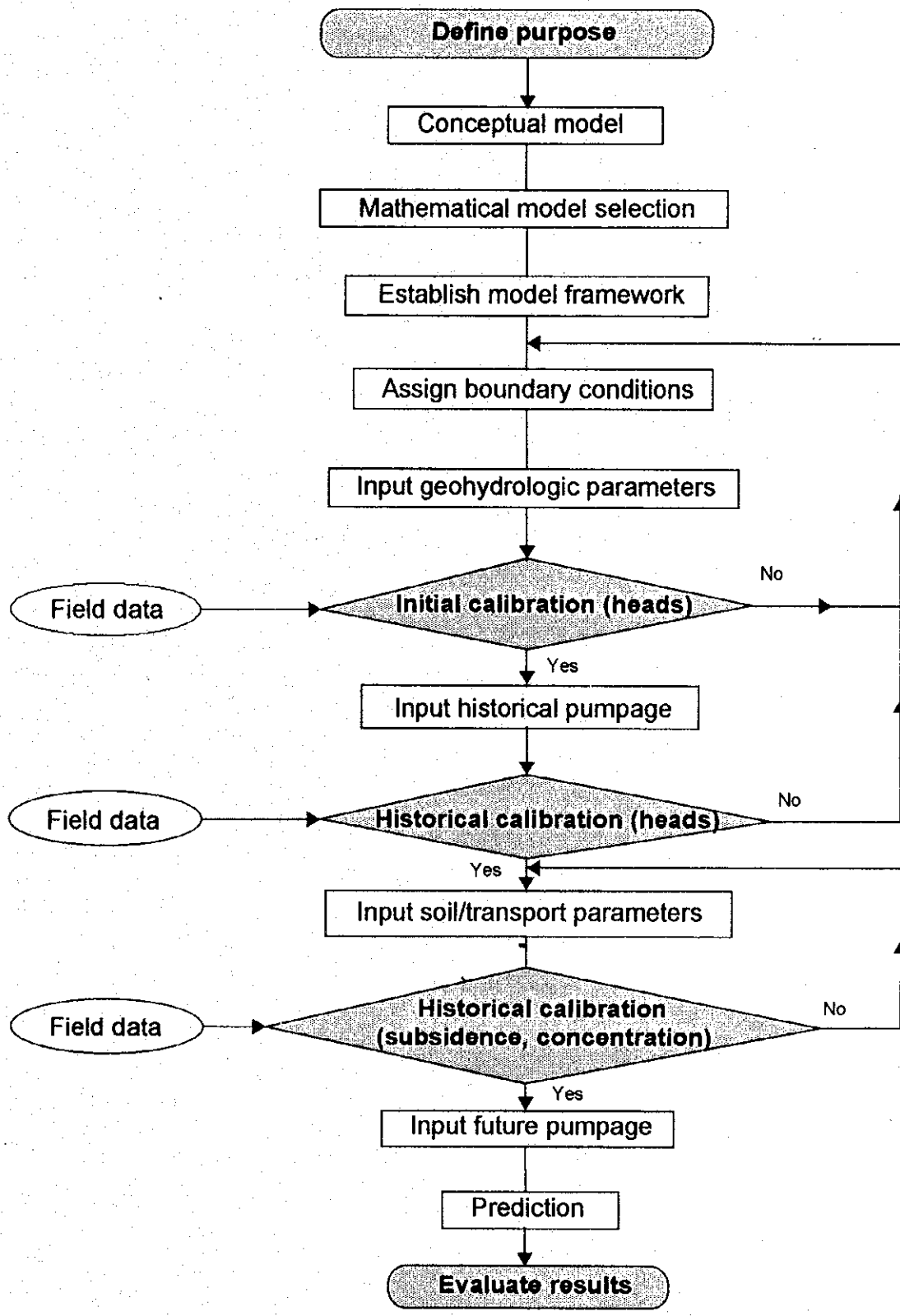


Figure 7.1.1	FLOW OF GROUNDWATER MODELING
THE STUDY ON MANAGEMENT OF GROUNDWATER AND LAND SUBSIDIENCE IN THE BANGKOK METROPOLITAN AREA AND ITS VICINITY	
JAPAN INTERNATIONAL COOPERATION AGENCY (JICA)	KOKUSAI KOGYO CO., LTD.



7.2 3-D Groundwater Flow and Land Subsidence Model

7.2.1 Model Concept

The digital model used for the Study is a three-dimensional groundwater flow model (MODFLOW program) and a land subsidence model (SUBPRO-1 program). Groundwater flow in a groundwater basin is by nature three-dimensional. Thus, the three-dimensional model is the best suited to simulate groundwater flow.

It was difficult, however, to simulate three-dimensional groundwater flow given the complexity of the structure of a groundwater basin, the inadequacy of input data, and the limitations of numerical solution techniques and memory capacity of a computer. But, since the USGS MODFLOW model, "A Three-Dimensional Finite-Difference Ground-Water Flow Model" by Michael G. McDonald and Arlen W. Harbaugh has been updated and faster personal computers become popular, the MODFLOW is the most widely used groundwater flow model in the world.

A graphical preprocessor and postprocessor, that is known as PM (PROCESSING MODFLOW), is used before running MODFLOW to input data and to avoid serious input errors. The required input parameters are listed on the display. The model size of the latest MODFLOW is only limited by the number of cells in a model layer. A layer can consist of 15,000 cells and the model can have up to 80 layers and 1,000 stress periods.

The SUBPRO-1 program was developed by the Study Team. The program can compute consolidation of clayey soils by considering thickness of clay, volume compressibility at loading and unloading, and changes in piezometric heads. SUBPRO-1 uses computed piezometric heads by MODFLOW as input data. Then soil consolidation of each aquifer unit is calculated at each time step. Total land subsidence values are obtained by totaling each layer's consolidation.

7.2.2 Groundwater Flow Equation

The three-dimensional movement of groundwater of constant density through porous earth material may be described by the partial-differential equation:

$$\frac{\partial}{\partial x} \left(K_{xx} \frac{\partial h}{\partial x} \right) + \frac{\partial}{\partial y} \left(K_{yy} \frac{\partial h}{\partial y} \right) + \frac{\partial}{\partial z} \left(K_{zz} \frac{\partial h}{\partial z} \right) - W = S_s \frac{\partial h}{\partial t} \quad (7.2.1)$$

where

K_{xx} , K_{yy} , and K_{zz} are values of hydraulic conductivity along the x, y, and z coordinate axis, which are assumed to be parallel to the major axes of hydraulic conductivity (LT^{-1});

h is the potentiometric head (L);

W is a volumetric flux per unit volume and represents sources and/or sinks of water (T^{-1});

S_s is the specific storage of the porous material (L^{-1}); and

t is time (T).

In general, S_s , K_{xx} , K_{yy} , and K_{zz} may be functions of space ($S_s = S_s(x,y,z)$, $K_{xx} = K_{xx}(x,y,z)$, etc.) and W may be a function of space and time ($W = W(x,y,z,t)$); equation (7.2.1) describes groundwater flow under nonequilibrium conditions in a heterogeneous and anisotropic medium, provided the principal axes of hydraulic conductivity are aligned with the coordinate directions.

Equation (7.2.1), together with specification of flow and/or head conditions at the boundaries of an aquifer system and specification of initial head conditions, constitutes a mathematical representation of a groundwater flow system. A solution of equation (7.2.1), in an analytical sense, is an algebraic expression giving $h(x,y,z,t)$ such that, when the derivatives of h with respect to space and time are substituted into equation (7.2.1), the equation and its initial and boundary conditions are satisfied. A time-varying head distribution of this nature characterizes the flow system, in that it measures both energy of flow and the volume of water in storage, and can be used to calculate directions and rates of movement.

Except for very simple systems, analytical solutions of equation (7.2.1) are rarely possible, so various numerical methods must be employed to obtain approximate solutions. One such approach is the finite-difference method, wherein the continuous system described by equation (7.2.1) is replaced by a finite set of discrete points in space and time, and the partial derivatives are replaced by terms calculated from the differences in head values at these points. The process leads to systems of simultaneous linear algebraic difference equations; their solution yields values of head at specific points and times. These values constitute an approximation to the time-varying head distribution that would be given by an analytical solution of the partial-differential equation of flow.

7.2.3 Land Subsidence Equation

The SUBPRO-1 program uses the consolidation theory to compute land subsidence. The compression of soil can be obtained by:

$$\Delta S = m_v \cdot b \cdot \Delta p \quad (7.2.2)$$

where, ΔS is soil consolidation, m_v is volume compressibility at loading, b is thickness of soil, and Δp is change in consolidation load. The rebound at unloading can be calculated by:

$$\Delta S = m_v' \cdot b \cdot \Delta p \quad (7.2.3)$$

where, m_v' is volume compressibility at unloading. In this case, Δp should have a negative sign so that ΔS is also shows a negative value. The value of Δp can be obtained from the computed piezometric heads. From equations (7.2.2) and (7.2.3), consolidation or rebound at a period between two (2) time steps is computed.

It is known that the values of m_v and m_v' vary with consolidation process. Therefore, relation between volume compressibility and consolidation pressure should be examined.

7.2.4 Required Input Data and Output Data

The required input data for the MODFLOW program are as follows:

for simulation control

- Type of simulation (steady-state or transient)
- Time unit of model data
- Number of stress period (time step) (for transient simulation)
- Length of stress period (for transient simulation)
- Number of time steps within a stress period (for transient simulation)
- Multiplier for length of time steps (for transient simulation)

for model grid

- X and Δx of cells
- Y and Δy of cells
- Position and landmarks
- Z of layers
- Top and bottom elevations of each layer
- Aquifer type of each layer
- Anisotropy factor (T_{yy}/T_{xx}) of each layer
- Boundary array of each layer (active, inactive, constant-head)
- Wetdry conditions (options)

for aquifer properties

- Porosity
- Specific storage
- Hydraulic conductivity
- Vertical hydraulic conductivity or vertical leakance
- Initial piezometric heads

for optional packages

- Well discharge or recharge by layer and by time step
- Drainage River
- Evapotranspiration
- General-head boundary
- Recharge
- Stream-aquifer relation

for solver selection

- Strongly Implicit Procedure (SIP) parameters
- Slice-Successive Overrelaxation (SSOR) parameters
- Preconditioned Conjugate Gradients 2 (PCG2) parameters

for output control

- Piezometric heads
- Drawdowns
- Volumetric budget
- Cell-by-cell flow
- Output files

- Output frequency

The output data from MODFLOW are computed piezometric heads, drawdown, volumetric budget, and cell-by-cell flow. These output data are available at each time step. The PM programs can convert these data from unformatted files into ASCII type files.

The land subsidence model (SUBPRO-1) requires following input parameters:

- Piezometric heads
- Volume compressibility (m_v)
- Ratio of m_v/m_v'
- Thickness of clay

The output data from SUBPRO-1 are:

- Computed consolidation of each layer at each time step
- Cumulative consolidation over time by layer
- Total land subsidence

7.2.5 Model Assumptions

The MODFLOW program assumes that hydrogeologic parameters such as hydraulic conductivity, specific storage, and leakance are not affected by changes in piezometric heads. Also, the program needs to assume that those parameters and boundary conditions do not change over time.

The SUBPRO-1 assumes that a consolidation process is completed within a time step.

7.2.6 Model Grid

The study area covers a part of the Lower Central Plain. The detailed hydrological study has been concentrated in the study area. However, it is necessary to consider the hydrogeologic conditions of the Lower Central Plain to simulate basin-wide regional groundwater flow. The merits to take a model domain up to the basin boundaries are to reflect the structures of the groundwater basin in the model and to increase reliability of simulation at marginal area of the study area. For instance, it is difficult to assign proper boundary conditions at the margin if only the study area is taken as a model domain, because the aquifers continue up to the outside of the study area and, especially near the northern boundary and the western boundary of the study area, the groundwater flow in outer area affects the groundwater flow in the study area. Therefore, the Study Team has taken the model grid as shown in Figure 7.2.1.

The grid size in the study area is fixed as 2km x 2km. The grid in the outside area varies from 2km x 4km to 16km x 16km in size as increasing size with increasing distance from the study area. A total number of modeled grids in one (1) layer is 2,860 (55 rows x 52 columns). The number of grids in the study area is 1,600.

The model is divided into ten (10) layers based on the hydrogeological classification and the memory size of the personal computer. The total number of 3-D cells is 28,600 (55 rows x 52 columns x 10 layers). The structure of the 3-D model is given in Figure 7.2.2. The top layer is an unconfined aquifer (UC), which is not confirmed from the field investigations. However,

this layer is needed for the model to express almost constant levels of surface water existing on the Bangkok Clay, otherwise a constant head boundary must be assigned to Bangkok Soft Clay then the heads in the clay cannot be simulated. The Bangkok Soft Clay (BC) is taken as an independent layer because the clay contributes to the land subsidence significantly in the study area. The aquifer units of Bangkok Aquifer (BK) to Pak Nam Aquifer (PN) are based on the hydrogeological classification studied in the previous stage. The units include not only sand and gravel facies but also silt and clay facies. The Stiff Clay of Bangkok Clay (Moh *et al.*, 1969) is significantly older than the Soft Clay (AIT, 1980) and its physical properties are quite different from the Soft Clay so that the Stiff Clay is treated as a member of Bangkok Aquifer in the model.

7.2.7 Boundary Conditions

Appropriate boundary conditions must be specified for numerical calculation based on the hydrogeologic information. At first, the extent of each aquifer unit was defined based on the geological studies done in the previous stage. Figure 7.2.3 shows a schematic profile of the Bangkok aquifer system and the concept of the 3-D model applied to the aquifer system.

According to the geological information, Bangkok area is underlain by Bangkok Clay (BC), but the extent of the clay is limited by Ayutthaya on the north, by Nakhon Nayok on the northeast, and by Nakhon Pathum on the west (AIT, 1980). The schematic geological diagram of the Lower Central Plain made by the Study Team indicates that the area from Ayutthaya to Chai Nat is underlain by the sediments of Ayutthaya Delta and Chai Nat Delta which can be correlated to the Bangkok Aquifer (BK). The eastern and western marginal areas of the Lower Central Plain are underlain by fan deposits and middle terrace deposits, which can be correlated to Phra Pradaeng (PD) Aquifer and Nakhon Luang (NL) Aquifer. The higher terrace deposits in those areas can be correlated to Nonthaburi (NB) Aquifer. On the other hand, the sediments of Sam Khok (SK) Aquifer to Pak Nam (PN) Aquifer do not have outcrops. The schematic profile of Figure 7.2.3 (a) was made based on the above information with considering the depths to the bedrock.

The geologic settings of the Bangkok aquifer system were conceptually modeled as shown in Figure 7.2.3 (b). An unconfined layer (UC) at the top was created on the BC layer to make the top of BC layer constant head. Some recharge shall be given to the cells of BK, PD, and NB layers where those layers are outcropping. The layers from SK to PN are bounded by the bedrock.

The areal boundaries of the aquifer units are shown in Figures 7.2.4 and 7.2.5. The NB layer is most widely distributed in the modeled area up to the bedrock outcrops. The extent of PN layer is limited by the bedrock structure.

The cells located out of the boundary in each layer are treated as inactive cells in the model. Constant head boundary condition is assigned to the entire active cells of UC layer. Also the constant head boundaries are given to the active cells located in the southernmost row (row No. = 55) within the Gulf of Thailand for each layer. The constant flow boundary is assigned to the active cells at northernmost row in NB layer because the layer continues toward north. Rest of the boundaries in each layer are treated as no-flow boundaries.

After the model calibration, the constant head boundaries were extended to the upstream areas of BK to NB layers where each layer occurs just below the ground surface. The cells in this area were previously identified as the recharge cells, but the reliable recharge rate were not able to be given due to lack of data and variation of the vertical hydraulic conductivity.

7.2.8 Hydrogeologic Parameters

(1) Top and bottom elevations

Top and bottom elevations of each layer are prepared from a ground elevation map and the bottom depth map of each aquifer unit. The data of ground elevation in the study area were obtained from the latest elevation of the DMR and RTSD benchmarks. It is noted that the elevation of benchmarks is generally higher than the original ground elevation. For instance, the measuring point of the DMR benchmarks is about 30 cm higher than the ground surface. However, it is difficult to determine the exact ground elevation because the height varies from station to station. Thus, the elevation of benchmark is regarded as the ground elevation. The elevations of the outer area were read from the 1:50,000 scale toposheets and the 1:250,000 scale geological maps. Figure 7.2.6 shows the ground elevation in the modeled area.

Then the top and bottom elevations of each layer except UC and PN layers were determined. The top elevation of UC layer was given by

$$(\text{Top elevation of UC}) = (\text{ground elevation}) + 1\text{m} \quad (7.2.4)$$

The bottom elevation of UC is the same as ground elevation. The bottom elevation of PN aquifer was given as -600m uniformly.

Figure 7.2.7 shows the isopach of Bangkok Soft Clay (BC) prepared from borehole data and lithologic logs of the DMR monitoring wells. Figures 7.2.8 to 7.2.11 show the bottom depths of BK, PD, NL, and NB aquifers. These maps were based on the aquifer classification done by the Study Team in the previous stage. The bottom depth maps of SK, PT, and TB aquifers (Figures 7.2.12 to 7.2.14) were prepared from the hydrogeological profiles made by the DMR (1987) and the hydrogeological profiles made by the Study Team. The aquifer classification was extended to the outside of the study area by using the lithologic logs listed on the database, then the top and bottom elevations for each aquifer in the modeled area were obtained.

From the top and bottom elevation data, the MODFLOW calculates the thickness of each aquifer unit by cell during the computation.

(2) Type of each layer

An Aquifer type must be specified for each layer. The unconfined aquifer type was assigned to UC layer. The confined aquifer type was assigned to the rest.

(3) Porosity

For the simulation of steady state flow, porosity is not required by MODFLOW. However, porosity is required by MODPATH program, which is the subprogram of MODFLOW for the calculation of the flow velocities, and, therefore, this parameter is required by MODFLOW input program, PM. The porosity value of 0.05 was uniformly given to the model.

(4) Specific storage

Although the Block-Centered Flow (BCF) Package of MODFLOW program requires dimensionless storage coefficient values in each layer of the model, however, it is only needed to specify specific storage values for each cell in PM. Then PM converts the specific storage value into dimensionless storage coefficient by multiplying the layer thickness of the cell.

It is common that the values of storage coefficient obtained from pumping tests take a wide range of variation, however, Walton (1970) suggested the range of storage coefficient values in confined aquifers varies between 1.0E-3 and 1.0E-5 for all soils and the range varies between 5.0E-5 and 1.0E-2 in productive aquifers. Therefore, the initial storage coefficient of each layer except UC and BC was assumed to be 1.0E-3, then this value was converted into specific storage by dividing the value by the thickness of the cell.

The specific storage values of BC were computed by following equation from the volume compressibility values obtained from consolidation tests:

$$Ss = m_v \cdot \gamma_w / 10 \quad (7.2.5)$$

where, Ss is specific storage (1/m), m_v is volume compressibility (cm^2/kgf), and γ_w is unit weight of water (g/cm^3). Details of estimating appropriate volume compressibility values shall be mentioned in the later section. The specific storage values of UC were based on the values of BC.

It is noted that equation (7.2.5) indicates the actual value of specific storage may not be constant when soil consolidation occurs. For example, if land subsidence occurs due to the drop of piezometric level, the volume compressibility may be changed. This will cause changes in specific storage, however, the MODFLOW program does not consider this phenomenon.

(5) Hydraulic conductivity

The parameter of transmissivity is the most important parameter for the model. PM will compute transmissivity from horizontal hydraulic conductivity (or permeability) by multiplying the layer thickness. An anisotropy factor (T_{yy} / T_{xx}) can be specified in the model.

Generally, transmissivity values are obtained from pumping tests. The Study Team collected previous pumping tests' data and carried out pumping tests at the newly constructed monitoring wells. However, the number of pumping tests and obtained aquifer parameters are still inadequate to evaluate regional aquifer characteristics. Therefore, the transmissivity values by aquifer were obtained from the hydrogeological information and specific capacity data of the production wells listed on the database. The method of estimating transmissivity is as follows:

- a) Classify production wells by aquifer using screen depths.
- b) Compute specific capacity value.
- c) Estimate apparent transmissivity from specific capacity using well data.
- d) Estimate permeability from apparent transmissivity and screen length.
- e) Compute clay content of each aquifer unit.
- f) Compute transmissivity of aquifer facies from estimated permeability, clay content, and isopach.

- e) Compute hydraulic conductivity for MODFLOW input by dividing transmissivity of aquifer facies by thickness of layer.

The production wells having screen length and production test data were used to compute specific capacity. The aquifer name of each well was identified by the bottom depth maps. Figure 7.2.15 shows the distribution of specific capacity values by aquifer with a logarithmic average and a range of the standard deviations. Figures 7.2.16 to 7.2.23 show the distribution of specific capacity for BK aquifer to PN aquifer with locations of the production wells.

Transmissivity values of the production wells were estimated by following three (3) methods:

- Unsteady-state estimation
- Steady-state estimation
- Estimation method by Logan (1964)

If the well has the data of discharge, drawdown, pumping time, and well radius, the specific capacity is given by the approximate nonequilibrium equation without well loss in confined aquifers presented by Cooper and Jacob (1946), that is:

$$Sc = \frac{Q}{s} = \frac{4\pi T}{2.30 \log(2.25Tt/r^2S)} \quad (7.2.6)$$

where, Sc is specific capacity (m^2/d), Q is well discharge (m^3/d), T is transmissivity (m^2/d), t is pumping duration (day), r is well radius (m), and S is storage coefficient (dimensionless). If S can be assumed as mentioned before, T can be obtained by solving Equation (7.2.6) numerically.

The steady-state estimation was used for the wells not having pumping time. The equilibrium equation for confined aquifers developed by Thiem (1906) is written as:

$$T = \frac{Q \ln(r_2/r_1)}{2\pi (s_1 - s_2)} \quad (7.2.7)$$

where, s_1 (m) and s_2 (m) are drawdowns of piezometric level at distances r_2 (m) and r_1 (m), respectively. Klimentov (1967) gave an empirical equation for computing the radius of influence as below:

$$r_2 = 2s \sqrt{T} \quad (7.2.8)$$

where, s (m) is drawdown in a well having well radius r (m). Changing from natural to common log base and substituting Equation (7.2.8) in Equation (7.2.7), Sc can be written as:

$$Sc = \frac{Q}{s} = \frac{5.46T}{\log(4Ts^2/r^2)} \quad (7.2.9)$$

Then, T can be obtained by solving Equation (7.2.9) by some numerical methods.

If the well has only the value of specific capacity, following equation presented by Logan (1964) was used to estimate transmissivity:

$$T = 1.22 Sc \quad (7.2.10)$$

The estimated transmissivity can be called as "apparent transmissivity", because the estimated transmissivity describes the ability of the perforated portion of the aquifer to transmit water. After obtaining the apparent transmissivity of the well by the said methods, the permeability k value was computed based on the definition of transmissivity given by:

$$k = T / b \quad (7.2.11)$$

where, b is the screen length. Figure 7.2.24 shows the distribution of estimated permeability by aquifer. Figures 7.2.25 to 7.2.32 show the distribution of estimated permeability by aquifer.

The clay content maps of BK aquifer to NL aquifer were prepared based on the lithologic logs of the DMR monitoring wells and some production wells. The clay content was computed by:

$$(\text{Clay content}) = \frac{(\text{total thickness of clay beds})}{(\text{aquifer thickness})} \times 100 (\%) \quad (7.2.12)$$

In case the layer is sandy clay, a value of 0.7 was multiplied to the thickness. Similarly, a value of 0.3 was used to multiply the thickness when the layer is clayey sand. The clay content maps of NB to TB aquifers were prepared based on the lithologic logs of production wells, because the DMR monitoring wells do not penetrate NB aquifer. Figures 7.2.33 to 7.2.39 show the aquifer thickness (isopach) of BK aquifer to TB aquifer. The distributions of clay content for BK aquifer to TB aquifer are shown in Figures 7.2.40 to 7.2.46.

The thickness of aquifer facies such as sand and gravel in each aquifer unit was then computed as follows:

$$(\text{Thickness of aquifer facies}) = (100 - \text{clay content} (\%)) \times (\text{isopach}) / 100 \quad (7.2.13)$$

Then the transmissivity of the whole aquifer facies was computed for each cell by:

$$(\text{Transmissivity of aquifer facies}) = (\text{thickness of aquifer facies}) \times (\text{permeability}) \quad (7.2.14)$$

The transmissivity of clay beds can be neglected due to the small values of permeability, meaning that the estimated transmissivity of aquifer facies can represent the transmissivity of the aquifer unit. Figures 7.2.47 to 7.2.54 show the finally estimated transmissivity of BK aquifer to PN aquifer. For PN aquifer, although the bottom depth is not confirmed from the field data, the elevation up to -600m was taken into account.

For MODFLOW input, the estimated transmissivity values were converted to hydraulic conductivity values by dividing the transmissivity by the layer thickness.

The hydraulic conductivity of BC layer was estimated from the permeability obtained from the consolidation tests as follows:

$$k = c_v \cdot m_v \cdot \gamma_w / (1E+5) \quad (7.2.15)$$

where, k is permeability of clay (m/d), c_v is coefficient of consolidation (cm^2/d), m_v is volume compressibility (cm^2/kgf), and γ_w is unit weight of water (g/cm^3). Figure 7.2.55 shows the distribution of clay permeability by aquifer unit. The obtained hydraulic values for BC layer were also given to UC layer.

(6) Vertical hydraulic conductivity or vertical leakance

The MODFLOW needs an input data set of vertical hydraulic conductivity or vertical leakance to calculate the vertical groundwater flow terms. If the data set type is selected as "vertical hydraulic conductivity", PM calculates the vertical leakance with the equation:

$$\frac{1}{L} = \frac{d_1/2}{k_{fv,1}} + \frac{d_2/2}{k_{fv,2}} \quad (7.2.16)$$

where, L is vertical leakance (1/day), $k_{fv,1}$ and $k_{fv,2}$ are vertical hydraulic conductivity of the upper aquifer and the lower aquifer (m/d), d_1 and d_2 are thicknesses of the upper aquifer and the lower aquifer (m). Actually, the leakance value is one of the unknown parameters from the field investigations, so the tentative values were estimated from the method mentioned below, then the appropriate values were identified from the model calibration.

It was already mentioned that each layer of the model consists of sandy facies and clayey facies except BC and UC layers. These facies beds occur alternately in the layer. So the average vertical hydraulic conductivity of the layer was computed based on the thickness and the permeability of each facies by the equation:

$$\log(k'_{av}) = [b_s \cdot \log(k'_s) + b_c \cdot \log(k'_c)] / b \quad (7.2.17)$$

where, k'_{av} is average vertical hydraulic conductivity of the layer (m/d), k'_s and k'_c are vertical hydraulic conductivities of sandy facies and clayey facies (m/d), b_s and b_c are thicknesses of sandy facies and clayey facies (m), and b is the total thickness of the layer. The values of k'_s and k'_c were estimated from Figures 7.2.24 and 7.2.55 with considering the effect of sedimentary structure, which may reduce vertical permeability values comparing with the horizontal permeability values.

(7) Initial piezometric heads

The initial piezometric heads of UC and BC layers for the initial steady-state calibration were given as the ground elevation shown in Figure 7.2.6. The initial heads of the other layers were assigned to be 0m in elevation. For the historical calibration for a period from 1983 to 1992, the computed heads by the steady-state calibration were input as the initial heads.

(8) Recharge rate

The recharge cells were identified based on the boundaries of the layers. A tentative recharge rate was given to the cells as 5% of annual precipitation. However, as a result of model calibration, it was found that unrealistic rise of piezometric level occurred at the cells where

relatively small values of hydraulic conductivity and/or vertical hydraulic conductivity were assigned. This is natural because recharge rate is greatly affected by soil conditions, such as infiltration rate, soil moisture, field water holding capacity, etc. In other words, the recharge rate may vary from place to place. Therefore, it is needed for accurate recharge assignment to investigate surface soil conditions, however, this was not done due to lack of data in the modeled area.

Instead of assigning the recharge rate, constant head boundary was assigned to the cells representing the recharge area. The piezometric levels at these cells were assumed to be the same as the ground elevation.

(9) Volume compressibility

The SUBPRO-1 needs a data set of volume compressibility at loading (m_v) and volume compressibility at unloading (m_v') for each layer. The values of compressibility were obtained from the consolidation tests done by the Study Team. Figure 7.2.56 shows the distribution of volume compressibility by aquifer unit. It is noted that the volume compressibility value of each sample was taken at the hydrostatic pressure, because the value changes over the loading steps. It is also noted that the identification of the preconsolidation pressure is difficult from deeper samples. Figure 7.2.57 shows the relation between sample depth and volume compressibility at the CI stations. The graph also indicates that the values sharply increase with decreasing depth. Figure 7.2.58 shows that the changes in volume compressibility with ground water pressure at Site-A. The graph indicates that the values of volume compressibility at shallower depths generally decrease with decreasing groundwater pressure. The changes of the values below 300m in depth are very small even though the groundwater level drops 70m. Therefore, it is suggested that the appropriate volume compressibility values should be given to the shallow layers considering the past and future groundwater pressures.

The m_v' value is smaller than m_v . The ratio of m_v/m_v' differs by aquifer unit and groundwater pressure. Based on the consolidation tests, appropriate ratios of m_v/m_v' were input to the model.

7.2.9 Model Calibration

(1) Preparation of pumpage data

Groundwater pumpage is one of the most important parameters for the simulation. The historical pumpage data of the Case-2, which were estimated from the database prepared by the Study Team, were used for the model calibration. Each production well can be located on the 1 km x 1 km grid system from its UTM coordinates. Then the pumpage of each model grid was computed horizontally by well location. The pumpage data cover not only the Study Area but also the whole seven (7) provinces.

Vertical distribution of the pumpage was carefully examined because it is very important for the 3-D model. The tapped aquifer(s) of each well was identified from its screen depth(s) or well depth by comparing with the bottom depth of each aquifer unit at the grid. If the well does not have the data of screen depth(s) and well depth, the tapped aquifer was estimated from the other wells located in the same grid. No wells extract groundwater from UC and BC layers. In case of the well tapped two (2) or more aquifers, the pumpage was divided by the number of tapped aquifers then distributed into each aquifer unit at the location.

A yearly pumpage data file and a quarterly data file for a period from 1983 to 1992 were prepared for the model calibration. The yearly data were used for the piezometric level calibration and the quarterly data were used for the calibrations of piezometric level and land subsidence. For preparing the quarterly pumpage data, the quarterly groundwater pumpage coefficients (QGPC) by type of user were used. It was also considered that the exact date of issuance for each private well.

The QGPC values were obtained from the wells having monthly pumpage data measured by flow meter. The average values of QGPC by user type are given in Table 7.2.1.

Table 7.2.1 AVERAGE VALUES OF QUARTERLY GROUNDWATER PUMPAGE COEFFICIENTS (QGPC)

TYPE OF USER	QGPC			
	Quarter 1 (Jan - Mar)	Quarter 2 (Apr - Jun)	Quarter 3 (Jul - Sep)	Quarter 4 (Oct - Dec)
PRIVATE WELLS				
DOMESTIC	1.053	0.965	1.049	0.933
PUBLIC	1.088	0.972	0.964	0.976
COMMERCIAL	1.032	1.052	0.960	0.956
INDUSTRIAL	0.989	1.027	0.993	0.991
PUBLIC WELLS	0.999	1.024	0.993	0.984

(Annual average pumpage = 1.000)

The QGPC values are generally higher in the first quarter and the second quarter, indicating that the pumpage in the dry season is larger than that in the rainy season.

Figures 7.2.59 shows the historical pumpage in the Study Area by aquifer unit from 1983 to 1992. The pumpage from NL aquifer is the largest throughout the period, that is 553,009 m³/day in 1983 and 640,850 m³/day in 1992. However, the percentage of NL aquifer to the total pumpage has decreased from 49.51% in 1983 to 43.27% in 1992. This is mainly due to the reduction of the MWA pumpage. The pumpage from NB aquifer is second largest, having 289,930 m³/day (25.96%) in 1983 and 396,054 m³/day (26.74%) in 1992. This pumpage was also decreased from 1985 to 1986 due to the reduction of the MWA wells. It is noted that the pumpage increasing rates of deeper aquifers have significantly increased. For instance, the pumpage from SK aquifer has increased from 11,559 m³/day (1.03%) to 55,257 m³/day (3.73%) for the period from 1983 to 1992. This indicates that the groundwater exploitation from the deeper aquifers has grown in the decade.

Figure 7.2.60 and Figure 7.2.61 show the distribution of groundwater pumpage from PD aquifer in 1983 and 1992, respectively. A heavily pumped grids can be seen from both the maps along the Chao Phraya River in Samut Prakan. Numbers of pumped grids have increased in the eastern parts of Samut Prakan, Bangkok, and Pathum Thani. The distribution of pumpage from NL aquifer in 1983 (Figure 7.2.62) indicates that the pumpage was concentrated in the central part of Bangkok in 1983. But by 1992, the heavily pumped grids has been spread to the wide areas in Samut Prakan, eastern Bangkok, Pathum Thani, and Samut Sakhon (Figure 7.2.63). However, the pumpage in the central Bangkok has decreased due to the phase-out of the MWA wells. The groundwater of NB aquifer was mainly used in the central part of Bangkok, Nonthaburi, and Pathum Thani in 1983 (Figure 7.2.64). But after

10 years, heavily pumped area has been spread to Pathum Thani, eastern Bangkok, Samut Prakan, and Samut Sakhon (Figure 7.2.65).

(2) Steady-state heads calibration

The steady-state calibration was carried out prior to the historical calibration. The purposes of the steady-state calibration are to understand model behavior, to check boundary conditions, to estimate approximate values of unreliable geohydrologic parameters, and to generate initial piezometric heads at the beginning of 1983 for each aquifer unit. The pumpage data in 1983 were used for the steady-state calibration.

A duration of 30 years was taken for the steady-state simulation using the constant pumpage rate with a time step of three (3) years. The reason of using the 30-year period is that the intensive groundwater development in the Study Area might be started from 1950s. The initial piezometric heads for the steady-state calibration were given as the ground elevation for UC and BC layers and 0m in elevation for the other layers.

During the calibration, the constant head boundaries were extended to the upstream areas of BK to NB layers where each layer occurs just below the ground surface. The cells in this area were previously identified as the recharge cells, but the reliable recharge rate were not able to be given due to lack of data and variation of the vertical hydraulic conductivity. The initial piezometric levels at these cells were assumed to be the same levels as the ground surface. The values of vertical hydraulic conductivity, which is one of the unreliable parameters in the Study Area, were modified. But hydraulic conductivity and specific capacity were kept at the originally estimated values.

As a result, it is found that the computed heads of BC to TB layers become almost stable within the first three (3) steps (= 9 years) starting from the initial piezometric heads. But the heads of PN layer continue to decline even though the declining rate is small. This is due to the small vertical hydraulic conductivity of PN layer, that allows small amount of upward leakage. The computed piezometric heads have reasonably matched with the actual piezometric heads. Then the heads were used as the initial heads for the historical calibration.

(3) Historical heads calibration

The annual historical pumpage data from 1983 to 1992 were input to the model. During the historical calibration, computed piezometric heads were carefully compared with the actual heads. Then the values of vertical hydraulic conductivity were modified by the trial-and-error method. The values of other parameters such as hydraulic conductivity and specific storage were not modified from the beginning. Because if several parameters were modified at the same time, the effect of each parameter change cannot be identified.

After modifying the parameters, the historical simulation was again carried out together with the steady-state simulation because the parameter change affects initial piezometric heads for the historical simulation. Therefore, simulation of 20 time steps, which consists of 10 time steps of steady-state simulation (1 time step = 3 years) and 10 time steps of historical simulation (1 time step = 1 year), was carried out.

The calibration of 3-D model is not easy even for modifying one (1) parameter because when the parameter value of a cell is modified, it will affect piezometric heads of not only horizontally surrounding cells but vertically surrounding cells. It is also needed to consider the

pumpage distribution of each aquifer unit near the cell as well as the possible range of variation of the parameter. This is like a complicated puzzle so that the logical calibration procedure is required. About 30 DMR monitoring stations were selected to carry out fine simulation by considering the monitoring period and location. Then reasonable parameter values were identified from upper aquifer units to lower aquifer units, because the top layer is maintained as the constant head boundary. It took about 50 times of historical simulation to obtain a good agreement between the actual heads and the computed heads at most of the points.

As a result, it was found that only modifying vertical hydraulic conductivity can almost match the computed heads with the actual heads. This means the originally input parameters of hydraulic conductivity and specific storage of each aquifer unit were reasonably estimated. There are some monitoring stations where the computed heads cannot be matched with the actual heads. There may be several reasons, for instance, screen position of the monitoring well is not exactly located at the aquifer unit, some problems in the well structure, influence of nearby pumpage, difference between actual pumpage and estimated pumpage, etc. In these cases, computed heads cannot match with the actual heads even though modifying hydraulic conductivity and/or specific storage. It is noted that the accuracy of pumpage data greatly affects the simulation results, especially in the piezometric level changes. There were several cases to estimate groundwater pumpage in the Study Area. However, it can be said that the Case-2 estimation, which was used for the model calibration, is the best estimate for the Study Area from the result of the simulation.

Finally, the 50 time steps historical calibration was carried out by input the quarterly pumpage data. The simulation consists of 10 time steps of steady-state simulation (1 time step = 3 years) and 40 time steps of historical simulation (1 time step = 91.25 days). The pumpage of the first quarter in 1983 was input to the former 10 time steps, then the quarterly pumpage data from 1983 to 1992 were given from 11th step to 50th step.

Figure 7.2.66 shows the comparisons between the simulated piezometric heads by the 50 time steps historical calibration and the actual piezometric heads at the DMR monitoring stations. The computed heads are reasonably simulated at the stations. The recoveries of piezometric levels at ST005 and ST055 are also revived by the model. Figures 7.2.67 to 7.2.69 show the comparisons between the simulated heads and actual heads of PD, NL, and NB aquifers at the end of 1992.

(4) Land subsidence calibration

The quarterly computed piezometric heads from 1983 to 1992 were used for the land subsidence model. It is important for land subsidence simulation to input quarterly piezometric heads data. Because in case of cyclic loading and unloading, the volume compressibility changes during the process of consolidation. From the results of the consolidation tests, the volume compressibility at the time of unloading (m_v') is only about 1/5 to 1/20 of that at the time of loading (m_v). Therefore, logarithmic average value of m_v and the typical value of the m_v / m_v' ratio of each clay was input to the model. The thickness of clay layer in each aquifer unit was given by each model grid from the isopach map and the clay content map of the aquifer unit.

During the calibration, the computed compression of each clay layer and the total computed land subsidence were checked. The changes in computed piezometric heads were also carefully examined to identify the parameters because the changes greatly affect the computed

compression. After several times of trial-and-error calibration, the values of m_v and m_v / m_v' were identified as shown in Table 7.2.2.

Table 7.2.2 IDENTIFIED VALUES OF m_v AND m_v / m_v'

Clay Layer	m_v (cm ² /kgf)	m_v / m_v'
BC	6.75E-02	20.0
BK	7.70E-03	10.0
PD	2.12E-03	10.0
NL	1.25E-03	10.0
NB	6.72E-04	10.0
SK	4.83E-04	5.0
PT	4.00E-04	5.0
TB	3.00E-04	5.0
PN	2.35E-04	5.0

It was found that the identified m_v and m_v / m_v' can satisfy the calibration without modifying the thickness of clay layers and without considering regional variation of m_v and m_v / m_v' values. Figure 7.2.70 shows the simulated land subsidence from 1983 to 1992. The actual land subsidence values for the period are not available because the RTSD did not conduct leveling survey from 1982 to 1984. However, the model can compute reasonable distribution of land subsidence comparing with the actual land subsidence distribution.

7.2.10 Predictions

(1) Future pumpage

Future piezometric levels can be predicted by using the calibrated simulation model. To predict future behavior of the model, nine (9) future pumping scenarios were prepared by considering several conditions and constraints. A 25-years prediction period was taken from 1993 to 2017. Each scenario was prepared based on the actual pumpage in 1992.

Before preparing each scenario, the trend of groundwater pumpage during the past five (5) years' period from 1988 to 1992 was examined by the following categories:

Type of user

- Private wells (DMR registered wells)
 - Domestic, Public, Commercial, and Industrial
- Public wells
 - ARD, DOH, IEAT, MWA, PWA, and PWD

Changwat

- Bangkok, Nonthaburi, Pathum Thani, Samut Prakan, Samut Sakhon, Phra Nakhon Si Ayutthaya, and Nakhon Pathom

Area

- The Study Area, Outside Area, and Whole Area

Then the basic pumpage data files in 1992 containing X and Y coordinates were prepared by the above category and by aquifer unit. It was assumed for preparing each scenario that the

present well locations (= grids) will not change in future and the pumpage distribution rate by aquifer unit at the grid is proportional to that in 1992.

The details of each scenario are mentioned in the Main Report. The summary of assumptions for the scenarios are presented in Table 7.2.3

The future simulation was carried out by input each scenario's pumpage data to the calibrated 3-D model. Since the accurate land subsidence prediction requires quarterly pumpage data, a data set of 100 time steps from 1993 to 2017 was prepared for each scenario based on the QGPC by type of user. The initial piezometric heads for the future simulation was prepared from the computed heads at the last time step of the final historical calibration.

(2) Scenario 1

The computed piezometric levels will straightly drop in the whole modeled area from 1993 to 2017. Figure 7.2.71 shows the simulated piezometric heads at the JICA monitoring stations. At Site-A (Lat Krabang, Bangkok), the simulated heads of NL aquifer and NB aquifer are below -80 masl in 2017. The piezometric level of NL aquifer at Site-B (AIT, Pathum Thani) drops below -190 masl in 2017. The piezometric levels of NL aquifer and NB aquifer at Site-C (Samut Sakhon) also drop straightly, located between -170 masl and -180 masl in 2017.

Figure 7.2.72 shows the simulated land subsidence at the JICA monitoring stations and the DMR office (central Bangkok). Severe land subsidence occurs at all the stations over the simulation period. The cumulative subsidence from 1993 to 2017 exceeds 200 cm at Site-C. The predicted land subsidence map by the year 2017 (Figure 7.2.73) shows a wide area in the Study Area will be subsided more than 50 cm. The subsidence more than 100 cm occurs in Samut Prakan, Bangkok, Pathum Thani, Samut Sakhon, and part of Nakhon Pathom. The areas subsided more than 150 cm are found in Samut Prakan and Samut Sakhon.

(3) Scenario 2

The piezometric levels in the MWA responsible area (Bangkok, Nonthaburi, and Samut Prakan) recover from 1998 due to the reduction of pumpage by the MWA Master Plan. Figure 7.2.74 shows that the piezometric level of NL aquifer at Site-A recovers about 15m from 1998 to 2017. In Pathum Thani, the piezometric levels recover when the surface water is supplied to the area, however, the piezometric levels again drop due to the increase of the groundwater demand. The simulated piezometric heads at Site-C show straight drop similar to Scenario 1, because Samut Sakhon is not covered by any water supply projects. The heads of NL aquifer and NB aquifer will be located between -160 masl and -170 masl in 2017.

Figure 7.2.75 shows that the subsidence at Site-A and the DMR office will almost stop from 1998. At Site-B, the subsidence becomes gentle from 1997 to 2003 with small rebound in 1997 and 2002 due to the changes in piezometric level. However, subsidence will again occur from 2004 then the rate of subsidence will be more than 3 cm/year. The subsidence at Site-C continues straightly, reaching 170 cm by the year 2017.

Figure 7.2.76 shows that the area subsided more than 50 cm by 2017 cannot be seen in major parts of Bangkok and Samut Prakan. The subsidence in central Pathum Thani ranges from 50 cm to 75 cm, which is smaller than that of Scenario 1. However, the subsidence in Samut Sakhon is still severe, showing more than 150 cm in the central part.